รายงานวิจัยฉบับสมบูรณ์

โครงการ การเพิ่มประสิทธิภาพด้วยการรวมระบบผลิตก๊าซเชื้อเพลิงจากชีวมวล และระบบเปลี่ยนรูปเพื่อผลิตก๊าซไฮโดรเจนและลดการปลดปล่อยก๊าซ CO_2 โดยการนำกลับมาใช้ใหม่

โดย

ดร. สุภวัฒน์ วิวรรธ์ภัทรกิจ สถาบันวิจัยพลังงาน จุฬาลงกรณ์มหาวิทยาลัย

ศ.ดร. สุทธิชัย อัสสะบำรุงรัตน์ ภาควิชาวิศวกรรมเคมี คณะวิศวกรรมศาสตร์ จุฬาลงกรณ์มหาวิทยาลัย

กันยายน 2559

Final Report

Performance improvement of integrated process of biomass gasification and reformer for green hydrogen production and reduction of CO_2 emission by utilization of recycled CO_2 as a gasifying agent

Supawat Vivanpatarakij,D.Eng — Energy Research Institute, Chulalongkorn University

Prof. Sutthichai Assabumrungrat — Department of Chemical Engineering, Faculty of Engineering, Chulalongkorn University

September 2016

สัญญาเลขที่ TRG5780233

รายงานวิจัยฉบับสมบูรณ์

โครงการ การเพิ่มประสิทธิภาพด้วยการรวมระบบผลิตก๊าซเชื้อเพลิงจากชีวมวล และระบบเปลี่ยนรูปเพื่อผลิตก๊าซไฮโดรเจนและลดการปลดปล่อยก๊าซ CO_2 โดยการนำกลับมาใช้ใหม่

โดย

ดร. สุภวัฒน์ วิวรรธ์ภัทรกิจ สถาบันวิจัยพลังงาน จุฬาลงกรณ์มหาวิทยาลัย

ศ.ดร. สุทธิชัย อัสสะบำรุงรัตน์ ภาควิชาวิศวกรรมเคมี คณะวิศวกรรมศาสตร์ จุฬาลงกรณ์มหาวิทยาลัย

สนับสนุนโดยสำนักงานกองทุนสนับสนุนการวิจัย
และจุฬาลงกรณ์มหาวิทยาลัย

กิตติกรรมประกาศ

รายงานการวิจัยนี้ได้รับการสนับสนุน จากสำนักงานกองทุนสนับสนุนการวิจัย (สกว.) ทุนส่งเสริมนักวิจัยรุ่นใหม่ประจำปี 2557 และ จุฬาลงกรณ์มหาวิทยาลัย ทุนเสริมรากฐานการวิจัย กองทุนรัชดาภิเษกสมโภช ปีงบประมาณ 2557 ซึ่งทางผู้วิจัยรู้สึกของพระคุณในการสนับสนุนทุนเพื่อใช้ในการศึกษาวิจัยนี้ และขอขอบพระคุณ ศ.ดร.สุทธิชัย อัสสะบำรุงรัตน์ ศูนย์เชี่ยวชาญเฉพาะทางด้านคาตาไลซีส และวิศวกรรมปฏิกิริยาที่ใช้ตัวเร่งปฏิกิริยา ภาควิชาวิศวกรรมเคมี คณะวิศวกรรมศาสตร์ จุฬาลงกรณ์มหาวิทยาลัย (นักวิจัยที่ปรึกษา) ที่ให้คำปรึกษาที่มีประโยชน์ต่อการศึกษาวิจัยในครั้งนี้

ดร.สุภวัฒน์ วิวรรธ์ภัทรกิจ

สถาบันวิจัยพลังงาน จุฬาลงกรณ์มหาวิทยาลัย

กันยายน 2559

Project Code : TRG5780233

Project Title : Performance improvement of integrated process of biomass gasification and reformer for green hydrogen production and reduction of CO_2 emission by utilization of recycled CO_2 as a gasifying agent

Investigator : Supawat Vivanpatarakij, D.Eng., Energy Research Institute, Chulalongkorn University.

Prof. Suttichai Assabumrungrat, Ph.D., Department of Chemical Engineering, Faculty of Engineering, Chulalongkorn University. (Mentor)

E-mail Address : supawat.v@chula.ac.th

Project Period : 2 Years

Using syngas as fossil fuel offers the benefit in term of suppress consumption of petroleum fuel. Gasification and reforming process can be used for syngas production. This work investigated the combined of gasifier and reformer process of charcoal with recycled CO_2. The investigation was carried on both simulation and experimental. The simulation results show that carbon conversion depended on operating temperature. The effect of O_2 in feed stream offered more heat obtained from process which optimum at O_2/B = 0.2. At higher S/B in feed stream led to more H_2 in syngas product. And the effect of CO_2/B feed ratio affect on both of CO_2 emr and syngas ratio. For feed ratio O_2/S/CO_2/B = 0.2/1/1/1 offered the highest Cold Gas Efficiency (CGE) of 0.742. From experimental study, the operating temperature of 800 ºC was observed for the highest carbon conversion. For the effect of Ni/SiO_2 catalysts, increasing Ni% loading offered more product gas due to the reforming reaction of gas product. Varying of O_2/S/CO_2/B feed ratio showed in similar trend of product gas mole fraction to the simulation result. For condition of CO_2/B ratio = 0, provided the highest for syngas yield. However, using CO_2 was beneficial in reducing GHG emissions and adjusting syngas ratio.

Keywords : biochar gasification, CO_2 reforming and Synthesis gas production

รหัสโครงการ: TRG5780233

ชื่อโครงการ: การเพิ่มประสิทธิภาพด้วยการรวมระบบผลิตก๊าซเชื้อเพลิงจากชีวมวล และระบบเปลี่ยนรูปเพื่อผลิตก๊าซไฮโดรเจนและลดการปลดปล่อยก๊าซ CO_2 โดยการนำกลับมาใช้ใหม่

ชื่อนักวิจัย: ดร. สุภวัฒน์ วิวรรธ์ภัทรกิจ สถาบันวิจัยพลังงาน จุฬาลงกรณ์มหาวิทยาลัย

ศ.ดร. สุทธิชัย อัสสะบำรุงรัตน์ ภาควิชาวิศวกรรมเคมี คณะวิศวกรรมศาสตร์ จุฬาลงกรณ์มหาวิทยาลัย

E-mail Address : supawat.v@chula.ac.th

ระยะเวลาโครงการ: 2 ปี

การใช้งานแก๊สสังเคราะห์สามารถช่วยลดการใช้งานเชื้อเพลิงจากปิโตรเลียม โดยแก๊สสังเคราะห์สามารถผลิตได้จากกระบวนการแก๊สซิฟิเคชันและเปลี่ยนรูป ในงานวิจัยนี้ศึกษาการประเมินผลของการรวมระบบแก๊สซิฟิเคชั่นและเปลี่ยนรูป ของถ่านไม้ด้วยการนา CO_2 กลับมาใช้ใหม่ โดยทาการศึกษาทั้งการใช้แบบจาลองและการทดสอบในห้องปฏิบัติการ จากการจาลองกระบวนการผลที่ได้พบว่า เมื่อเพิ่มอุณหภูมิทาให้ค่าร้อยละการเปลี่ยนแปลงของถ่านไม้สูงขึ้น การเพิ่มอัตราส่วนเชิงโมลของออกซิเจนต่อถ่านไม้ในสายป้อนที่เหมาะสมคือ 0.2 ทาให้ได้พลังงานจากระบบสูงที่สุด การเพิ่มอัตราส่วนเชิงโมลของไอน้าต่อถ่านไม้จะช่วยทาให้ได้ H_2 เป็นผลิตภัณฑ์มากขึ้น และการปรับอัตราส่วนเชิงโมลของ CO_2 ต่อถ่านไม้ สามารถช่วยปรับอัตราส่วนการปลดปล่อย CO2 และอัตราส่วนของ แก๊สสังเคราะห์ได้ด้วย สาหรับเงื่อนไขที่ใช้อัตราส่วน O_2/ไอน้า/CO_2/ถ่าน ไม้ เป็น 0.2/1/1/1 จะให้ค่าประสิทธิภาพของแก๊สผลิตภัณฑ์สูงที่สุดที่ 0.742 ในส่วนของการทาการทดลองศึกษาผลการใช้ตัวเร่งปฏิกิริยา พบว่าที่อุณหภูมิการทาปฏิกิริยา 800 องศาเซลเซียสจะทาให้ค่าร้อยละการเปลี่ยนแปลงของถ่านไม้สูงที่สุด ผลของการใช้ตัวเร่งปฏิกิริยาเป็น Ni/SiO_2 พบว่าเมื่อเพิ่มปริมาณของ Ni ในตัวเร่งปฏิกิริยาจะได้แก๊สผลิตภัณฑ์มากขึ้นเนื่องจากการเกิดปฏิกิริยา เปลี่ยนรูปของก๊าซขาออกมากขึ้น ส่วนผลการศึกษาอัตราส่วนการป้อนของ O_2/ไอน้ำ/CO_2/ถ่านไม้ ให้ผลเป็นไปตามแนวโน้มเดียวกันกับผลจากการจาลองกระบวนการ ที่อัตราส่วนการป้อน CO_2 ต่อถ่านไม้เป็นศูนย์ ส่งผลให้ค่าผลได้ของแก๊สผลิตภัณฑ์สูงที่สุด อย่างไรก็ตามการป้อนคาร์บอนไดออกไซด์เป็นการ ช่วยในการลดการปลดปล่อยก๊าซเรือนกระจกและสามารถปรับอัตราส่วนของแก๊สสังเคราะห์ได้

คำหลัก : การผลิตก๊าซเชื้อเพลิงจากถ่านไม้, การเปลี่ยนรูปด้วยคาร์บอนไดออกไซด์ และ การผลิตก๊าซสังเคราะห์

1. Introduction

1.1 Rationale

Global warming and energy crisis are among important issues. Biomass is well-known as renewable energy with high energy yield and to suppress consumption of petroleum [1]. Synthesis gas (syngas) consists of carbon monoxide and hydrogen. Controllable syngas ratio can be used in different applications such as electrical energy source [2, 3], fuel cell [4, 5] and other downstream processes [6, 7].

Gasification process can utilize many types of gasifying agent. Air is the cheapest gasifying agent but provides the low heating value of syngas due to impurity of nitrogen. Therefore, enriched oxygen in air leads to increase in heating value of syngas product [8]. Steam has been used as gasifying agent. The higher steam content and reaction temperature produce syngas product with more hydrogen yield [9, 10]. However, increasing steam and reaction temperature are required more energy to process. Carbon dioxide as a gasifying agent was recently presented the most benefit before emission to the atmosphere. Furthermore, using CO2 as gasifying agent offers several advantages such as producing more reactive char for better efficiency of gasification process, and adding CO2 involved in adjusting syngas ratio with more flexible for syngas application [11, 12].

Gasifier effluents are fed to reforming process for upgrading products. There are many types of reforming reactions. Steam reforming is a well-known technology that reforms light-hydrocarbons into syngas product. Higher steam as reforming agent offers higher H2 yield of syngas product due to steam reforming and water gas shift reaction [13]. Additionally, the advantage of steam reforming, fed excessive steam, is reducing coke formation. Although steam reforming is the most feasible and provides high hydrogen yield, but it is highly endothermic reaction and required heat for generating steam which causes high fuel consumption [14]. Dry reforming uses CO2 to reform light-hydrocarbon into syngas product. This reaction not only reduces

1.2 Objective

To investigate effect of using CO2 as gasifying agent on combined biomass gasification and catalytic reformer for hydrogen production

2. EXPERIMENTAL AND MODELING

Experimental and simulation methods were described in this chapter by divided into 3 sections. Section 2.1 explains feedstock preparation and characterization. Simulation of combined gasifier with reformer is described in section 2.2. Finally, details of reaction study are provided in section 2.3.

2.1 Materials preparation and characterization

2.1.1 Biomass

A charcoal was used for representing biomass, because it shows lower volatile matter than fresh sawdust [27]. Mangrove charcoal was chosen to represent as biomass in Thailand. The samples were sieved to get samples with mesh sizes between 16-20 mesh. Consequently, characterizations of charcoal were carried out to determine weight percentage of components (including carbon, hydrogen, nitrogen and oxygen) and percentage of physical properties (including moisture, volatile matter, fixed carbon and ash) by using ultimate and proximate analysis methods, respectively.

2.2 Simulation of combined gasifier and reformer

The simulation used Aspen Plus software. The main purpose was to find out the possible boundary of operating condition for experimental study.

2.2.1 Process description

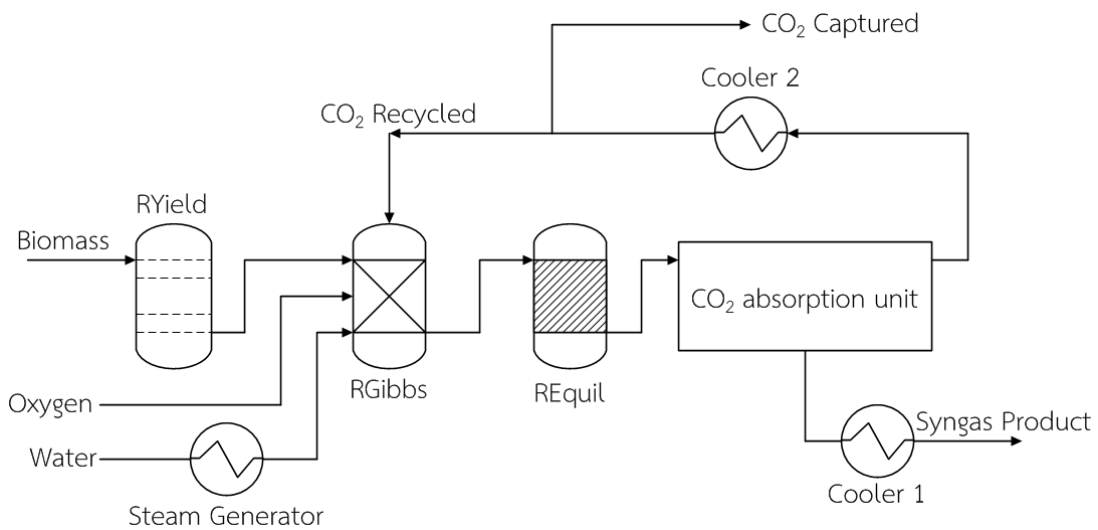

Figure 2.1 Process flow diagram of combined gasifier and reformer

Combined gasification with reforming system composes of gasifier, reformer and CO2 separation unit. Biomass represented by charcoal is used as feedstock for utilization with inlet reaction agents of steam and oxygen. Produced carbon dioxide is later recycled back to the process for use as reaction agent. Process flow diagram is illustrated in Figure 2.1 and conditions of feedstock and reaction agents are summarized in Table 2.1.

Table 2.1 Inlet conditions of feedstock and reaction agents

Feedstock	Charcoal
Inlet temperature of biomass and O_2	25 °C
Inlet temperature of CO_2	150 °C
Inlet temperature of steam	327 °C
Pressure	1 atm

Charcoal was fed to the gasifer, separated into two reactors (RGibbs and RYield). RYield reactor is used for breaking charcoal down to elements containing carbon, hydrogen, oxygen and nitrogen. Consequently, the elements are fed to RGibbs reactor for gasification process with other reaction agents. Subsequently, gasifier effluent is directly fed to reformer modeled by using a REquil reactor in order to upgrade syngas product. The product is treated in the CO2 absorption unit for eliminating CO2 out of the product stream, for this step heat required is 3 MJ/kg CO2 captured. Finally, the CO2 is recycled to RGibbs for use as reaction agents again. CO2 capturing stream is installed in order to adjust the CO2/Biomass feed ratio.

2.2.2 System modeling

Modeling of gasification process can be done by using each stoichiometric or non-stoichiometric approach, called Gibbs minimization approach. Set of reactions and extent of reaction are known parameters for the case of stoichiometric approach. For non-stoichiometric approach, only the expected product gas components are defined. Many researches confirm that the Gibbs minimization method give good agreement of results as the experimental results [47-49].

Charcoal used as unconventional component in Aspen Plus is fed to RYield reactor for breaking down to elements has input data as listed in Table 2.2. The high heating value of charcoal using the correlation provided by Channiwala and Parikh [49] is shown in Eq. 2.1.

$$HHV\ (MJ/kg) = 0.3491x_C + 1178.3x_H - 0.1034x_O \quad (2.1)$$

Carbon conversion of simulation process is calculated by Eq. 2.2.

$$\text{Carbon conversion} = \frac{(C_{in} - C_{out})}{C_{in}} \times 100 \quad (2.2)$$

Table 2.2 Input data of charcoal

Variable	Data
Feed rate	100 kg/h
Stream class	MIXCINC
Properties	PENG-ROB
Valid phases	Vapor-Liquid
Enthalpy	HCOALGEN (6 1 1 1)
Density	DCOALIGT

Table 2.3 Range of studied parameters

Gasifier temperature	200-800 °C
Reformer temperature	500-1,000 °C
O_2/Biomass ratio (O_2/B)	0-0.5
Steam/Biomass ratio (S/B)	0-1
CO_2/Biomass ratio (CO_2/B)	0-1

Table 2.3 shows the range of studied parameters including gasification temperature, reforming temperature, O2/B feed ratio, S/B feed ratio and CO2/B feed ratio. This work was simulated under isothermal condition. O2/B was set in the range of 0 to 0.5 for assuring the partial oxidation occurred. Figure 2.1, cooler 1 was installed to reduce temperature of syngas product to 30 °C and cooler 2 set for removing heat from CO2 stream in order to obtain the temperature at value of 150 °C. Long-chained hydrocarbon compounds are neglected for this work.

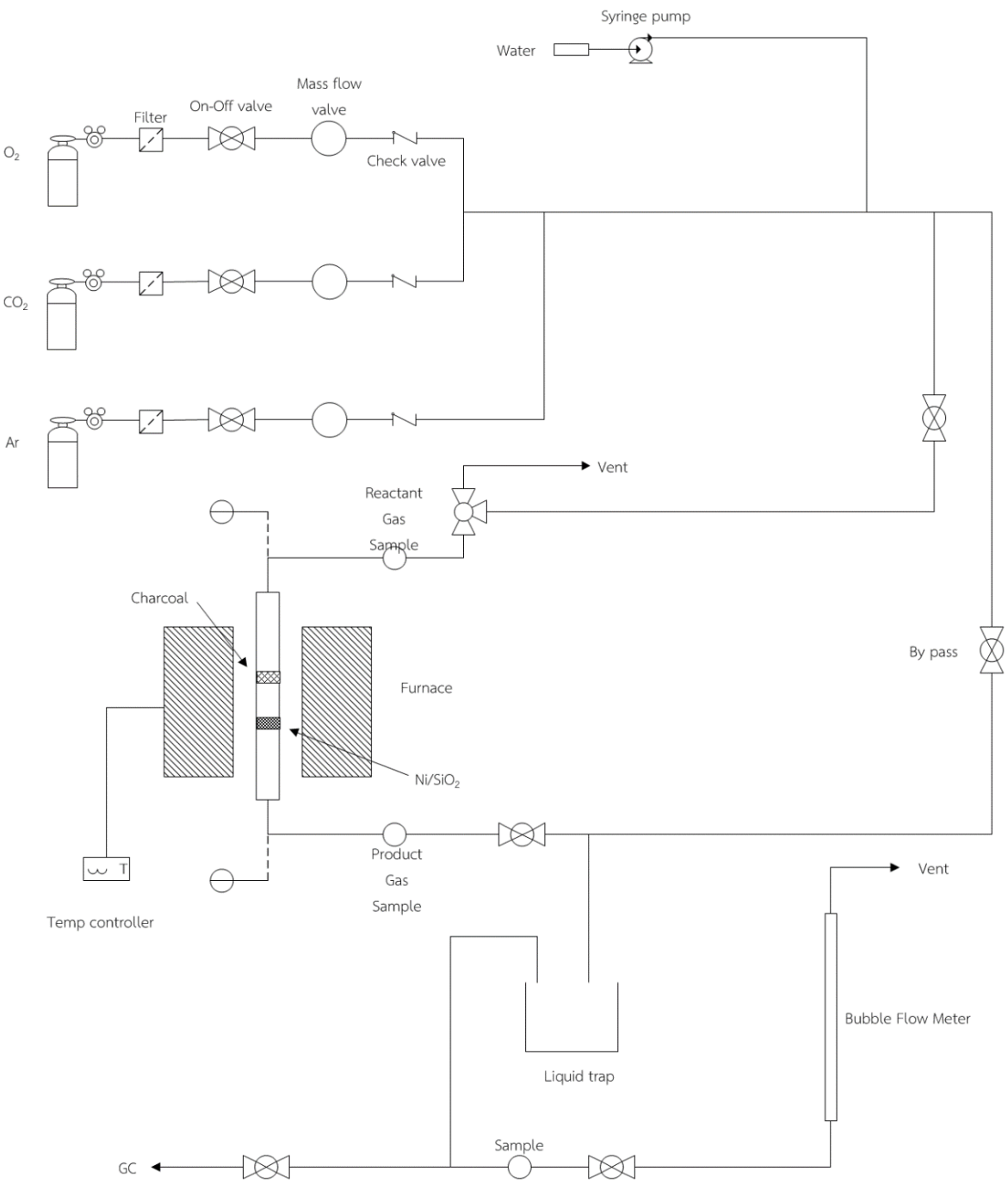

Figure 2.2 Schematic of reaction study

Table 2.4 Operating conditions

% Ni loading	5 – 15 %
Temperature	400 – 800 °C
Pressure	Atmosphere
O_2/Biomass ratio (O_2/B)	0-0.5
Steam/Biomass ratio (S/B)	0-2
CO_2/Biomass ratio (CO_2/B)	0-1.5

Table 2.5 Operating conditions of Gas Chromatography

Gas chromatography	Shimadzu GC
Detector	TCD
Carrier gas	Ar (purity 99.99%)
Column temperature	70 °C
Injector temperature	100 °C
Detector temperature	70 °C
Current	70 mA

2.3.2 Catalysts and characterization

Ni/SiO2 catalysts were used in this experiment with various percentages of nickel loading by 5%, 10% and 15%. Nickel(II) nitrate hexahydrate (Sigma-Aldrich) solution, dissolved with distillate water, is used as precursor for impregnation on the commercially available silica sand (SiO2) (Sigma-Aldrich) as supporter. Consequently, the catalysts were dried at 105 °C overnight in order to evaporate water. Subsequently, calcination was able to remove the volatile compound under condition of air with temperature of 500 °C for 4 hours.

Prepared catalysts were characterized by X-ray diffraction (XRD) techniques to observe the XRD peak pattern which indicated the presence of metal catalyst and support element using X-ray diffractometer SIEMENS D 5000. The results were shown in a range of 2θ of 20° and 80°.

BET surface area measurement (BET) technique was conducted by BET Micromeritrics ASAP 2020 using 0.1 g of sample to obtain surface area and pore volume of prepared catalysts.

Scanning Electron Microscope (SEM) is used for investigating the morphology and also measuring the particle size of prepared catalysts analyzed by Hitachi S-3400N with accelerating voltage of 15kV.

H2 temperature-programmed reduction (H2-TPR) was used for investigating the optimum reduction temperature of catalysts before using in the reaction study by Micrometrics Chemisorb 2750. Catalyst sample of 0.1 g was packed with quartz wool of 0.03 g in U-tube quartz reactor, then removed the moisture content from catalyst particle by using N2 gas with heating to 200 ºC and held for 1 hour. Subsequent, the catalyst was cooled down to ambient temperature and heated up to 800 ºC under 25 ml/min of 10% H2/Ar for temperature programmed reduction. Hydrogen gas used in this step was observed by thermal conductivity detector (TCD) and plot versus temperature.

Thermal gravimetric analysis (TGA) is used for analyzing the coke formation of spent catalysts. Using Mettler-Toledo TGA/SDTA for investigated the percentage of weight loss by carbon on catalysts combustion versus temperature.

2.3.3 Product analysis

Effect of reaction temperature was studied by controlling furnace temperature at 400 °C, 600 °C and 800 °C. Percentages of nickel loading on catalyst were varied at 5%, 10% and 15% in order to obtain the optimum condition for the following parameter. Finally, out of optimum %Ni loading and reaction temperature then the several of reaction agents to biomass feed ratio, O2/B, S/B and CO2/B, were studied.

Product gases were investigated using gas chromatography (TCD) equipment (detailed in Table 2.5). Carbon conversion is calculated using carbon balance of CO2, CO, CH4 and charcoal method by Eq. 2.5 [14]. H2 and CO yields from experimental were reported by proportion of total mole of H2 and CO to gram of biomass used by Eq. 4.6 [9].

$$\text{Carbon conversion (\%)} = \frac{\text{formation of } (CO + CO_2 + CH_4)}{\text{feeding of } (\text{Carbon} + CO_2)} \times 100 \tag{2.5}$$

$$\text{Yield (mol/gram-biomass)} = \frac{\text{mole of product gas (mole)}}{\text{biomass feed (gram)}} \tag{2.6}$$

3 RESULTS AND DISCUSSION

3.1 Charcoal characterization

In order to study the combined gasifier with reformer process, characterization of raw material charcoal was tested by proximate and ultimate analysis and the results are presented in Table 3.1. Data from proximate and ultimate analysis were used for this study in both of simulation and experiment.

Table 3.1 Proximate and ultimate analysis of charcoal

Proximate (wt%)	
Moisture	5.30
Volatile matters	36.26
Fixed carbon	56.40
Ash	2.05
Ultimate (wt%)	
C	66.46
H	4.37
O (balance)	29.14
N	0.03
High heating value (MJ/kg)[a]	50.581

[a] calculated using correlation proposed by Channiwala and Parikh [49]

3.2 Characterization of fresh catalysts

Before reaction test, characterization of catalysts were conducted by X-Ray Diffraction (XRD), BET surface area measurement, hydrogen temperature programmed reduction (H2-TRP) and Scanning Electron Microscopy (SEM).

3.2.1 X-Ray Diffraction (XRD)

The XRD peaks of Ni/SiO2 catalysts with varying loading percentage of Ni from 5%, 10% and 15% were illustrated in Figure 3.1. The diffraction peaks of NiO on catalysts were observed at degree of 37.2º, 43.3 º and 62.9 º for 3 types of catalysts as reported by Taufiq-Yap et al. [19] and Wang et al. [51]. NiO degree shows higher peaks with increasing of %Ni loading.

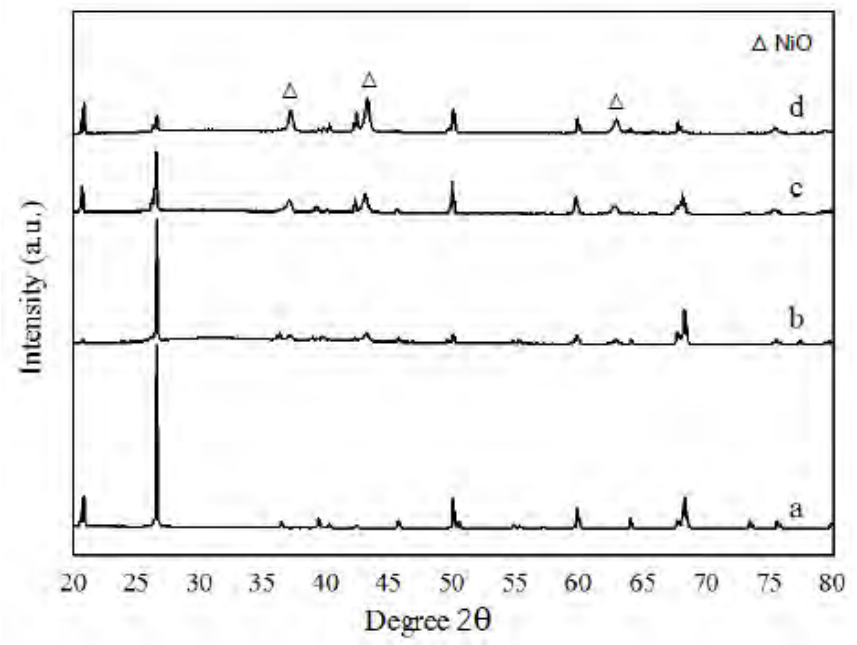

Figure 3.1 XRD patterns of SiO2 and Ni/SiO2 with various percentages loading

(a) SiO2, (b) 5%Ni/SiO2, (c) 10%Ni/SiO2 and (d) 15%Ni/SiO2

3.2.2 BET surface area measurement

Surface area results of catalysts are shown in Table 3.2. Increasing in %Ni loading on support results in reduction of surface area (SiO2 > 5%Ni/SiO2 > 10%Ni/SiO2 > 15%Ni/SiO2, respectively).

Table 3.2 Physical properties of catalysts

Catalysts	Surface area (m^2/g)
SiO_2	5.47
5%Ni/SiO_2	3.82
10%Ni/SiO_2	3.28
15%Ni/SiO_2	2.22

3.2.3 Hydrogen temperature programmed reduction (H2-TRP)

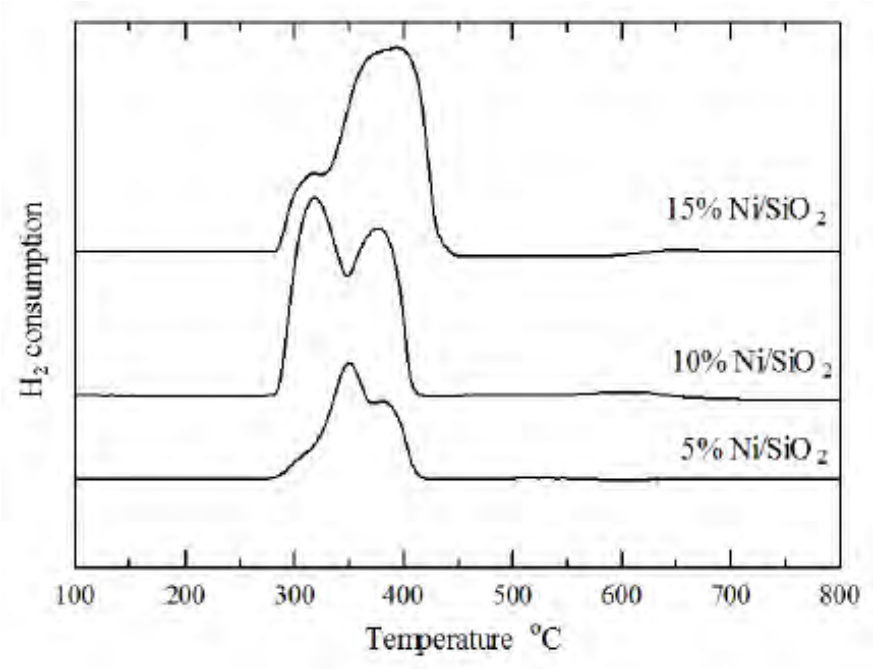

Figure 3.2 H2-TPR profiles of catalysts.

H2-TPR analysis was conducted for the catalysts. Reducibility of NiO on support was presented as TPR profile as shown in Figure 3.2. The main reduction peaks of catalysts were observed clearly for temperature around 350 ºC to 400 ºC. The results are in agreement with Taufiq-Yap et al. [19] and Wang et al. [51].

3.2.4 Scanning Electron Microscopy (SEM)

To understand the influence of %Ni loading on SiO2 support, catalysts were characterized using SEM as shown in Figure 3.3. The morphology of Ni/SiO2 with various %Ni loading was

observed and compared to SiO2. Higher %Ni loading shows higher of NiO sites as seen in Figure 3.3(d). 5%Ni/SiO2 displayed the slightly difference with SiO2 support as in Figures 3.3(a) and (b).

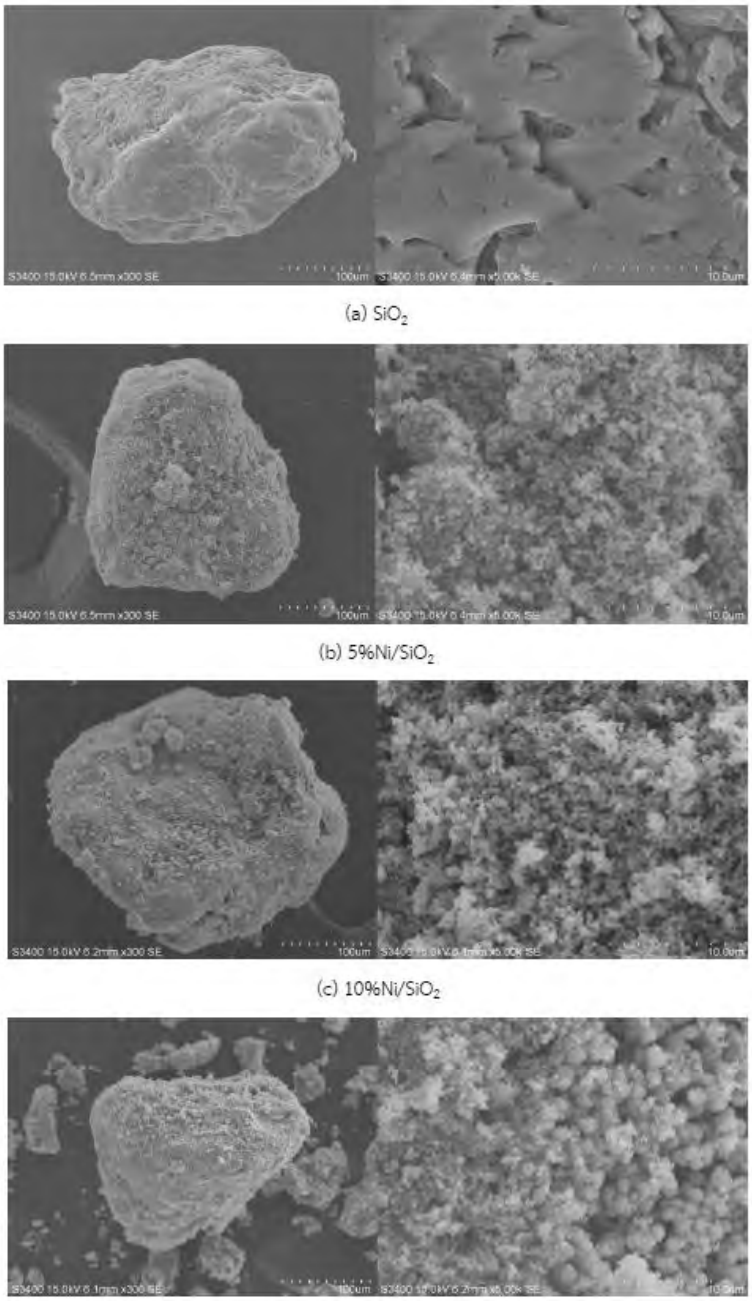

(a) SiO_2

(b) 5%Ni/SiO_2

(c) 10%Ni/SiO_2

(d) 15%Ni/SiO_2

Figure 3.3 SEM images of fresh catalysts.

3.3 Model validation

Before studying the simulation, the model was verified by comparing the gasifier model with Renganathan [12] and Chaiwatanodom [11]. The differences were less than 10%, revealing the good agreement of this model as shown in Table 3.3.

Table 3.3 Model validation of gasifier (biomass CH1.4O0.6, CO2/C = 0.5, P = 1 atm)

	[12]	[11]	This work	%error [12]	%error [11]
T = 800 °C					
yH_2	0.3070	0.3098	0.3108	1.23	0.32
yCO	0.6000	0.5978	0.5977	0.39	0.02
yCO_2	0.0980	0.0901	0.0892	8.99	1.01
yCH_4	0.0000	0.0430	0.0023	n/a	94.54[a]
T = 1000 °C					
yH_2	0.2900	0.3025	0.3036	4.68	0.35
yCO	0.6250	0.6241	0.6238	0.19	0.05
yCO_2	0.0810	0.0733	0.0726	10.38	0.97
yCH_4	0.0000	0.0587	0.0000	n/a	n/a
T = 1200 °C					
yH_2	0.2900	0.2943	0.2957	1.95	0.46
yCO	0.6500	0.6429	0.6424	1.18	0.08
yCO_2	0.0670	0.0628	0.0620	7.49	1.31
yCH_4	0.0000	0.0710	0.0000	n/a	n/a

[a] Neglect due to insignificant value

Model validation of reformer was also verified. Comparison of the model with Gopaul and Dutta [52] also showed a good agreement, confirmed by the difference less than 10% as shown in Table 3.4.

Table 3.4 Model validation of reformer (CH4/CO2 = 1.43, P = 1 atm)

	[52]	This work	%error [52]
T = 800 ºC			
H_2 (kmol/kmol biogas)	0.900	0.830	7.77
CO (kmol/kmol biogas)	0.630	0.690	9.52
CO_2 (kmol/kmol biogas)	0.036	0.039	8.33
CH_4 (kmol/kmol biogas)	0.020	0.018	10.00
T = 900 ºC			
H_2 (kmol/kmol biogas)	0.970	0.907	6.49
CO (kmol/kmol biogas)	0.705	0.770	9.22
CO_2 (kmol/kmol biogas)	0.010	0.011	10.00
CH_4 (kmol/kmol biogas)	0.008	0.007	8.75
T = 1000 ºC			
H_2 (kmol/kmol biogas)	0.990	0.903	8.78
CO (kmol/kmol biogas)	0.741	0.776	4.95
CO_2 (kmol/kmol biogas)	0.000	0.002	n/a
CH_4 (kmol/kmol biogas)	0.000	0.000	n/a

3.4 Thermodynamic analysis of combined gasifier and reformer process

The simulation results of combined gasifier and reformer process using various reaction agents are reported below.

3.4.1 Effect of gasifier temperature

The simulations were proceeded to study the conversion of carbon at different gasifier temperatures. Figure 3.4 illustrates that the gasifier temperature (Tg) of 600 ºC offers the maximum conversion of charcoal to reach 100%. Due to endothermic reaction of reverse boudouard and steam reforming, increasing reaction temperature leaded to higher conversion accordingly to standard Gibbs free energy changes of gasification reactions [37].

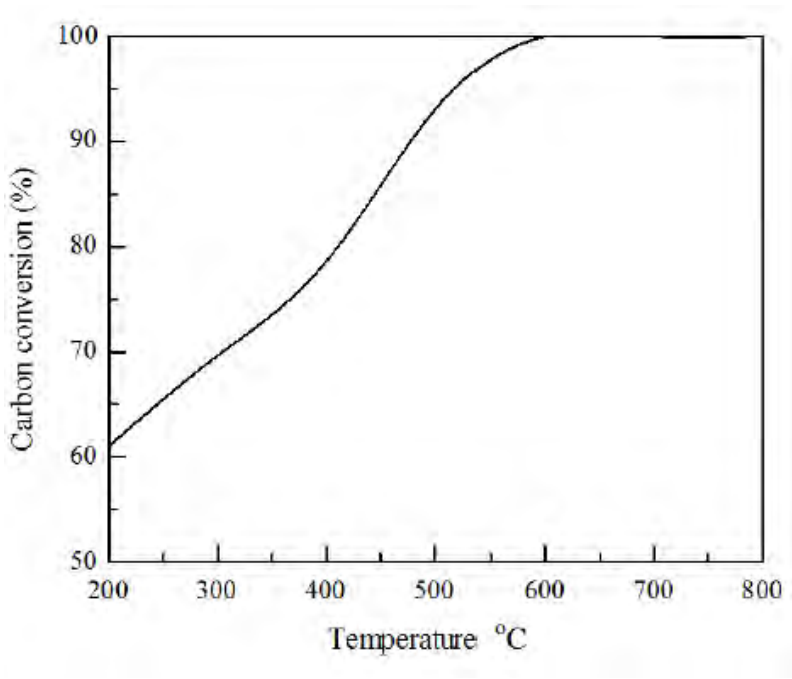

Figure 3.4 Effect of gasification temperature on carbon conversion (O2/B = 0.5, CO2/B and S/B = 1)

3.3.2 Effect of reformer temperature

Previously, the gasifier temperature (Tg) of 600 ºC offers the carbon conversion reaching maximum, this condition is used for studying the reforming temperature (Tr) parameter. Figure 3.5(a) shows the effect of reformer temperature on product gases composition, cold gas efficiency (CGE) and syngas ratio (H2/CO). Higher reformer temperature offers the lower trend of H2 and CH4 composition, but rising of CO. They are mainly explained by endothermic reverse water gas shift and methane reforming reaction. So, syngas ratio is presented in downtrend. CGE is reached the maximum value of 0.51 at 700 ºC of reformer. CO2 emr, the emission ratio of CO2 to atmosphere, also reduced with higher reformer temperature due to endothermic of reverse boudouard reaction. Total heat required for process is calculated by the difference between heat supplied to each unit in the process and enthalpy of syngas. The minus value means that there is net heat generated from the process. The total heat obtained from process increases with reformer temperature as illustrated in Figure 3.5(b).

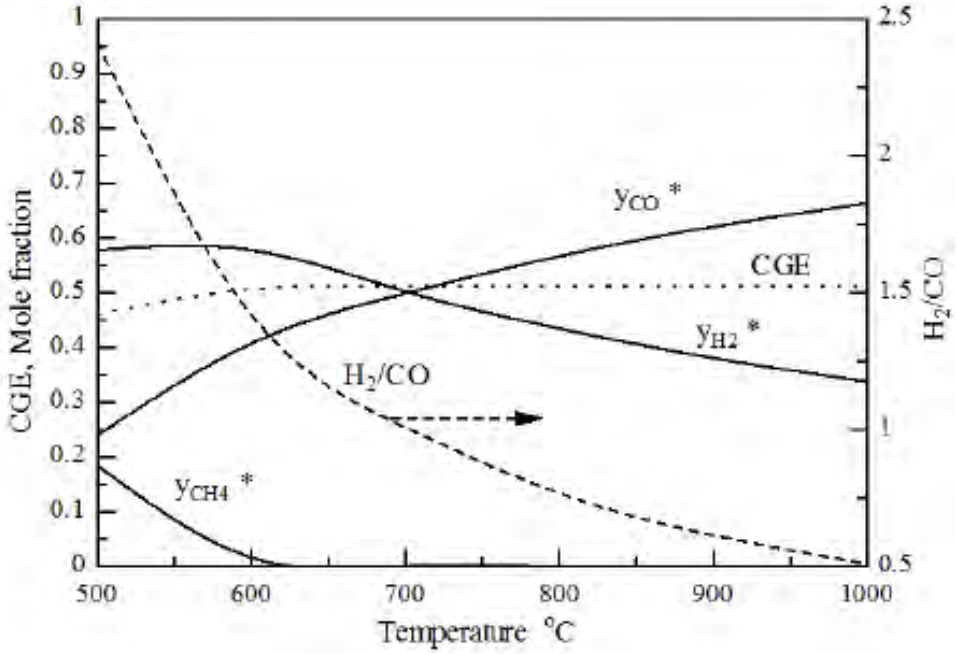

(a) Product gas compositions, CGE and H2/CO ratio Note *excluding H2O and CO2

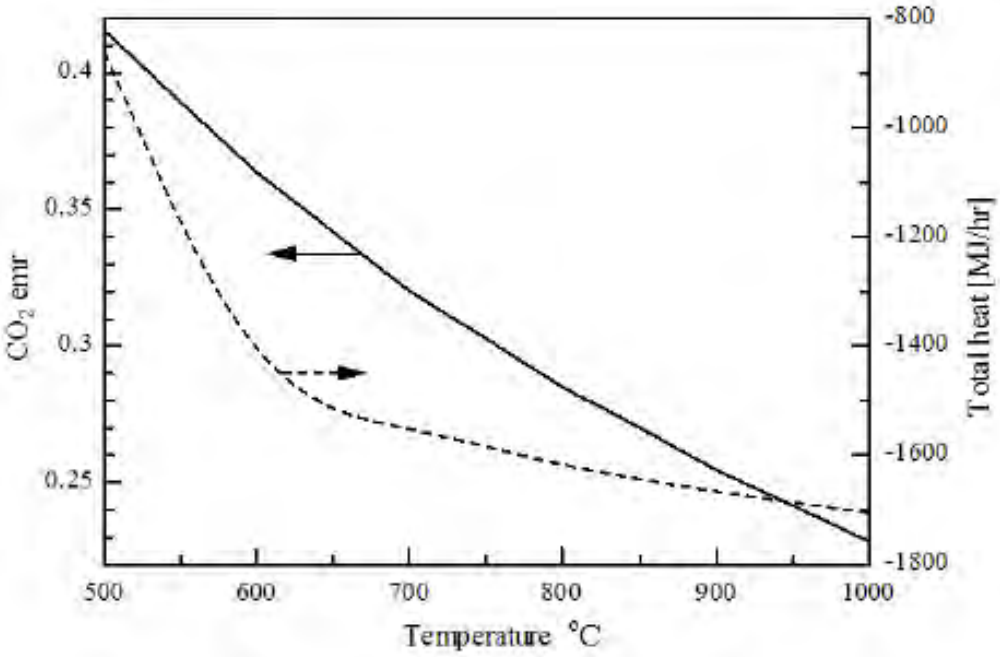

(b) CO2 emr and total heat

Figure 3.5 Effect of reformer temperature on (a) product gases and (b) CO2 emr and total heat (Tg = 600 ºC, O2/B = 0.5, CO2/B and S/B = 1)

3.3.3 Effect of O2/B feed ratio

Gasifier temperature (Tg) of 600 ºC and reformer temperature (Tr) of 700 ºC were used as standard condition for the next simulation part. S/B and CO2/B feed ratio were both fixed as 1 for studying the effect of oxygen feed ratio. O2/B feed ratio was used at maximum of 0.5 to make the partial oxidation reaction possible. CGE reached the maximum for the O2/B ratio of 0.2 then dropped with higher feed ratio because at higher O2, combustion reaction is more favorable than partial oxidation reaction. The product gases composition is reported in Figure 3.6(a). The CO2 emr value becomes higher with increasing O2/B ratio, and the total heat increased with presence of O2 due to exothermic reaction and optimum at O2/B ratio of 0.2 as displayed in Figure 3.6(b).

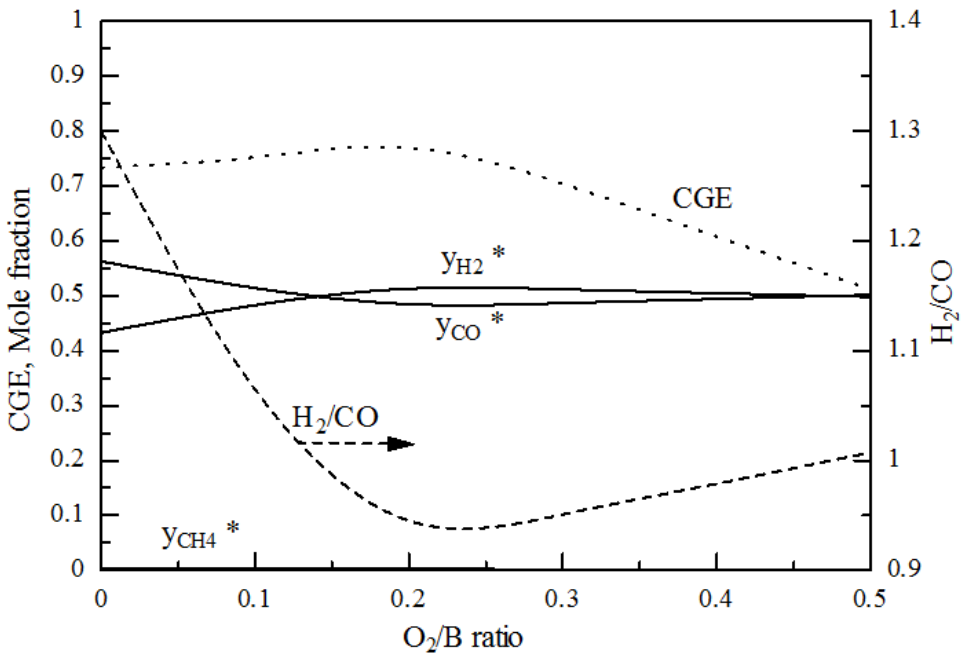

a) Product gas compositions, CGE and H2/CO ratio Note *excluding H2O and CO2

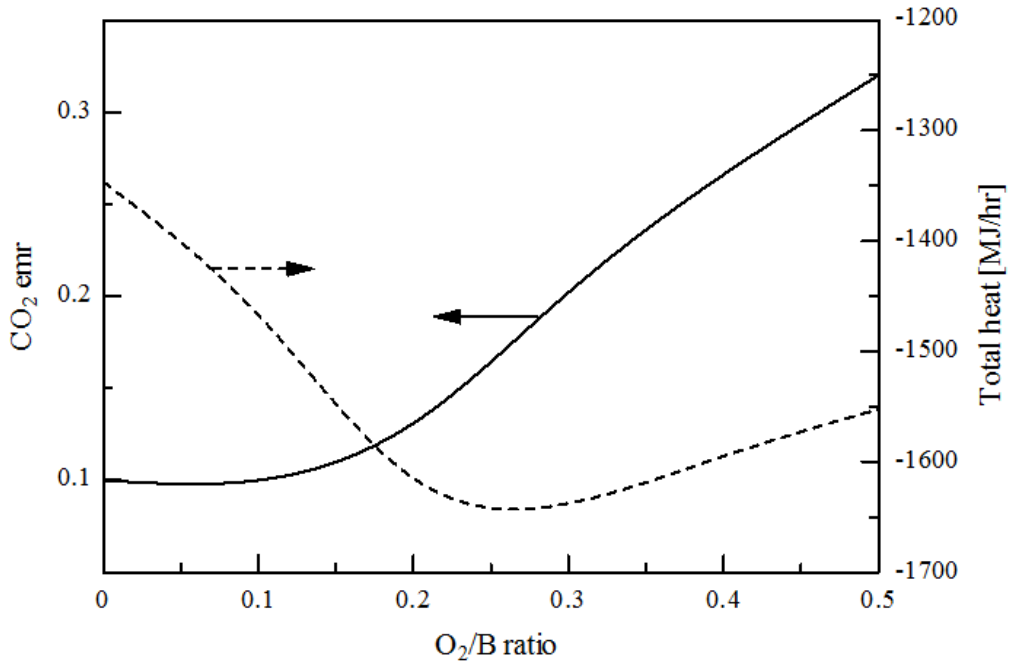

(b) CO2 emr and total heat

Figure 3.6 Effect of O2/B feed ratio on (a) product gases and (b) CO2 emr and total heat (Tg = 600 ºC, Tr = 700 ºC, CO2/B and S/B = 1)

3.3.4 Effect of S/B feed ratio

Figure 3.7(a) indicates the higher H2/CO ratio in the product with increasing molar S/B feed ratio from 0 to 1, agreeing with Wei et al. [10], because of steam reforming and water gas shift reaction. For S/B ratio approximately 0.4, CGE achieved the highest at 0.511 and stayed stable. CH4 was found to be insignificantly small amount. It can also indicate that water gas shift reaction plays an important role in increasing of CO2 composition, causing CO2 emr rising up from 0.21 to 0.32, this was also reported by Wei et al. [10]. Total heat obtained from process increased with introduced steam by feed ratio from 0 to 0.4, nevertheless, S/B feed ratio beyond 0.4 pulled down the heat obtained due to the increased demand for the steam generating unit as shown in Figure 3.7(b).

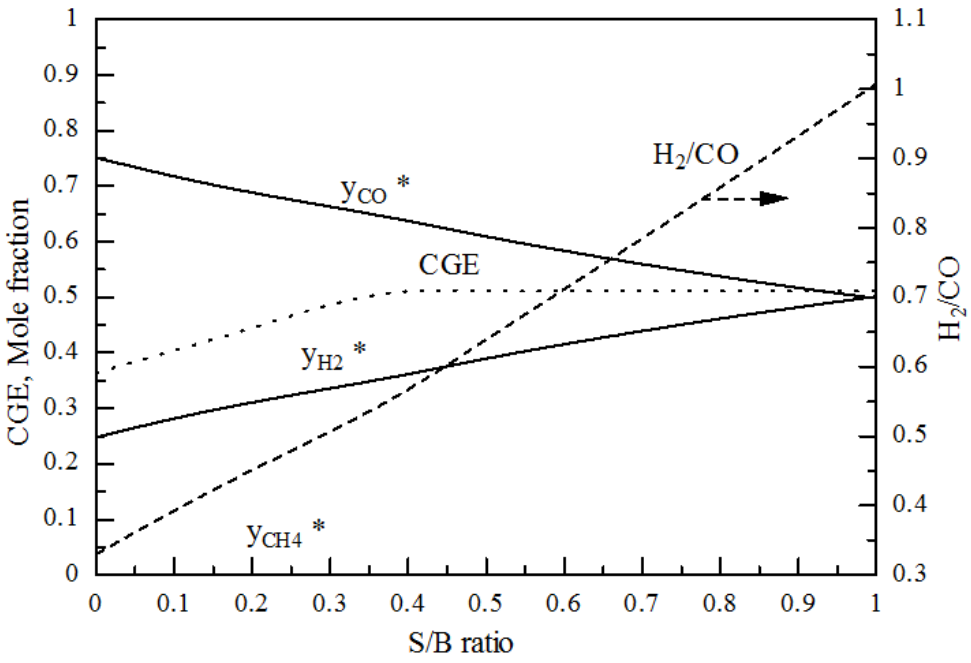

a) Product gas compositions, CGE and H2/CO ratio Note *excluding H2O and CO2

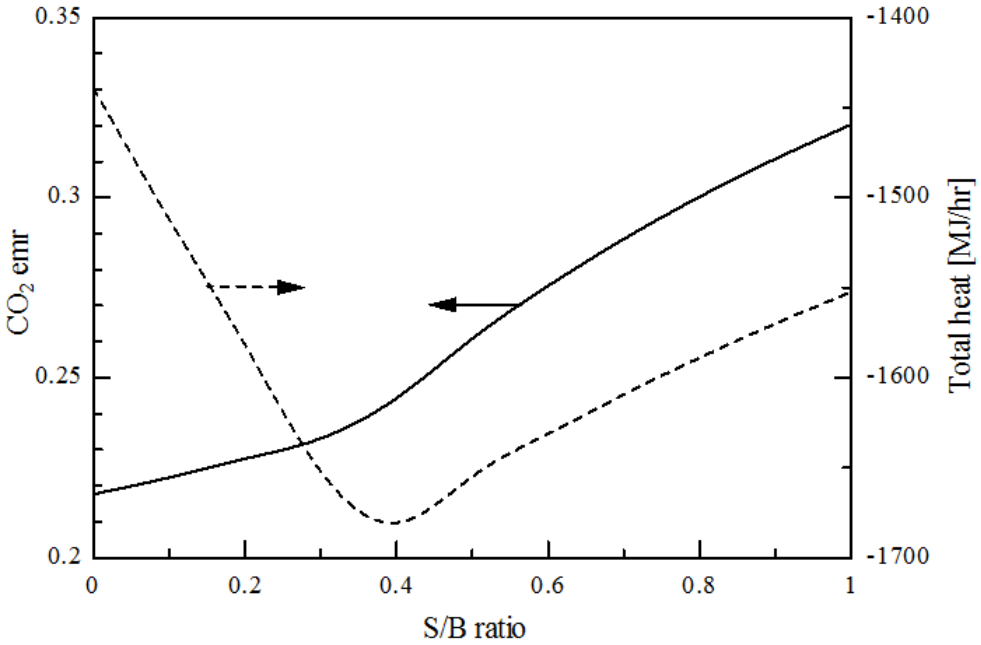

b) CO2 emr and total heat

Figure 3.7 Effect of S/B feed ratio on (a) product gases and (b) CO2 emr and total heat (Tg = 600 ºC, Tr = 700 ºC, CO2/B = 1 and O2/B = 0.5)

3.3.5 Effect of CO2/B feed ratio

This simulation part is investigated the effect of CO2/B ratio. This step is divided into sub-parts for studying the best condition of both O2/B and S/B affecting to CO2/B ratio.

Before investigating the effect of O2/B and S/B feed ratio on CO2/B, standard conditions of both O2/B and S/B were set as 0.5 and 1, respectively. The results are illustrated in Figure 3.8 as follows. For Figure 3.8(a), increasing in CO2/B ration offers lower of H2 with greater CO because higher CO2 in feed shifts the reverse boudouard reaction to produce more CO, similar to the reverse water gas shift reaction, resulting in higher and lower in constant rate of CO and H2, respectively. This results in a relatively constant CGE value at about 0.51 but the H2/CO ratio could be varied in a range of 1 - 1.9. The results are in good agreement of trend with Chaiwatanodom [11].

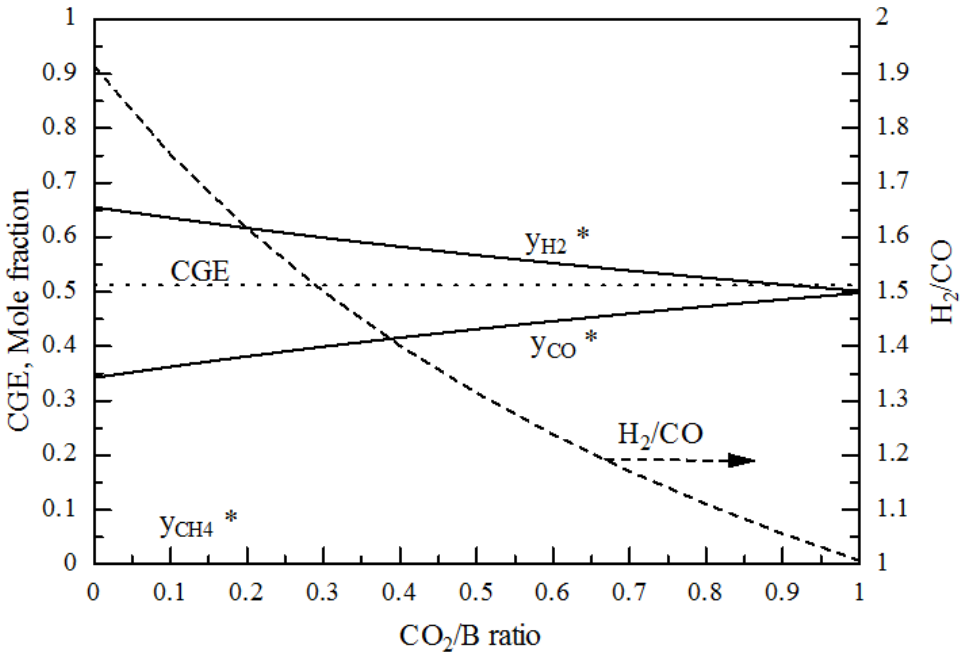

(a) Product gas compositions, CGE and H2/CO ratio Note *excluding H2O and CO2

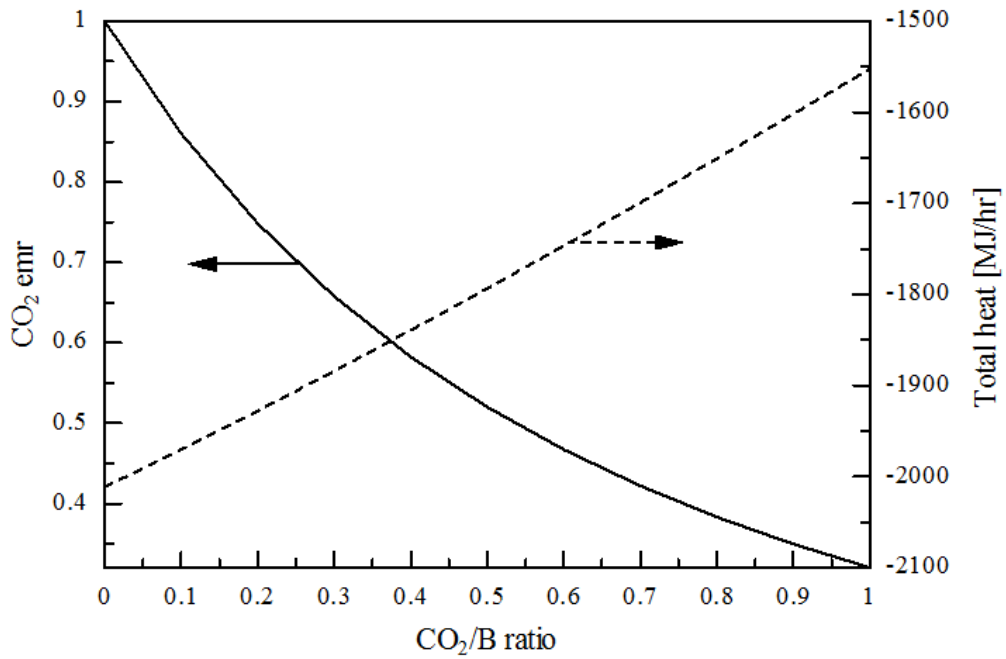

(b) CO2 emr and total heat

Figure 3.8 Effect of CO2/B feed ratio on (a) product gases and (b) CO2 emr and total heat (Tg = 600 ºC, Tr = 700 ºC, S/B = 1 and O2/B = 0.5)

The CO2 emr decreased from 1 to 0.42 when increasing CO2/B feed ratio from 0 to 1, indicating that more recycle of CO2 back to process can reduce the CO2 emission. However, heat obtained from the process also reduced from 2,011 MJ/hr to 1,552 MJ/hr by supplying to the CO2 capture and recycle processes as displayed in Figure 3.8(b).

The next sub-part focued on the effect of CO2/B ratio at the best condition of O2/B feed ratio of 0.2 with S/B = 1. The results are shown in Figure 3.9. Trends are almost similar to O2/B of 0.5. Except to CGE, the higher of CGE (indicated more efficiency of syngas product) obtained from O2/B ratio of 0.2 higher than O2/B ratio 0.5 by 0.51 to 0.77. Product gas compositions and syngas ratio are less difference from the previous condition as below in Figure 3.9(a).

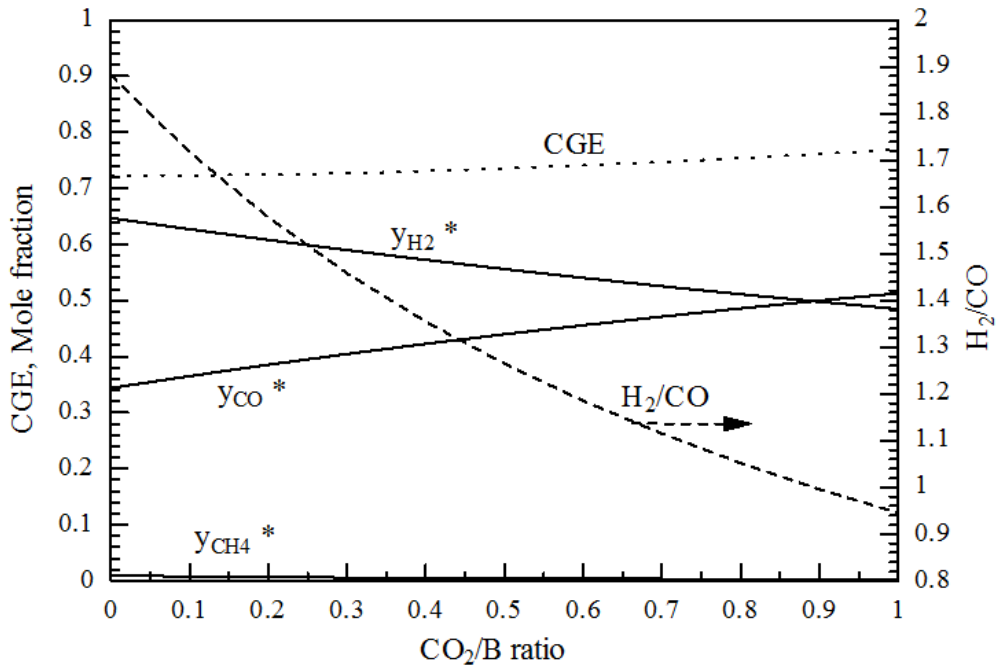

(a) Product gas compositions, CGE and H2/CO ratio Note *excluding H2O and CO2

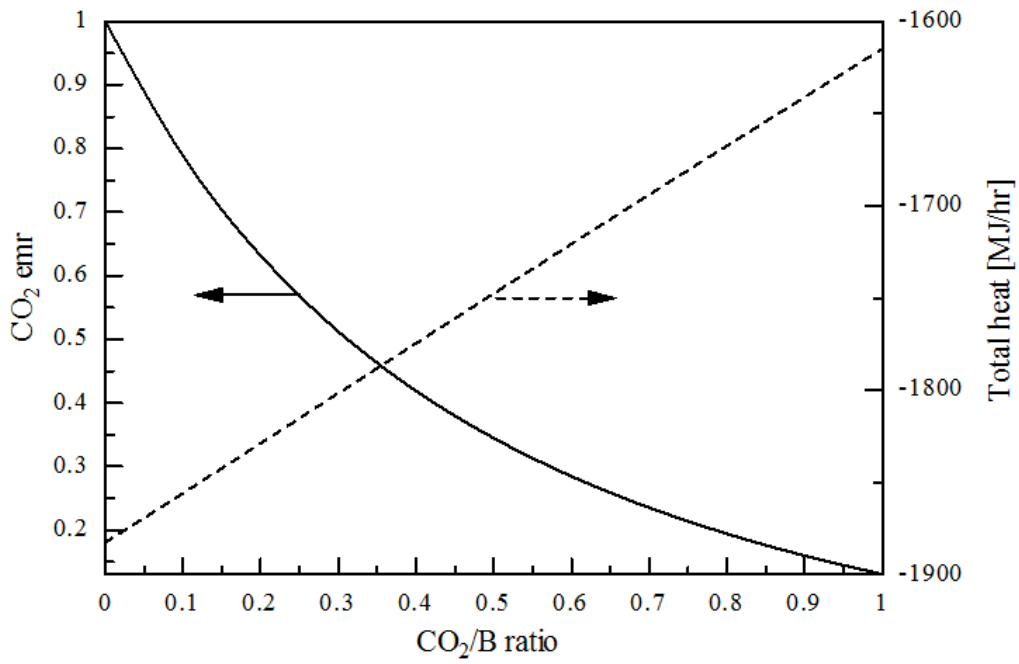

(b) CO2 emr and total heat

Figure 3.9 Effect of CO2/B feed ratio on (a) product gases and (b) CO2 emr and total heat (Tg = 600 ºC, Tr = 700 ºC, S/B = 1 and O2/B = 0.2)

For CO2/B nearly 1, the CO2 emr value of 0.13 is less than condition of O2/B = 0.5 because more O2 in feed stream produced more CO2 causing to more emission of CO2 from the

process. However, net heat which obtained in this case was lower than the previous condition for CO2/B ratio less than 0.8. This indicated that for O2/B ratio of 0.2 condition, the CO2/B ratio greater than 0.8 did not only offer high value of CGE and net heat obtained from process but also reduced in cost of O2 feed and also CO2 emission as shown in Figure 3.9(b).

Next sub-part is focused on the condition at the ratios of S/B = 0.4 and O2/B = 0.5. The product gas compositions, syngas ratio, CGE, CO2 emr and net heat which obtained from process were shown in Figure 3.10 as follows.

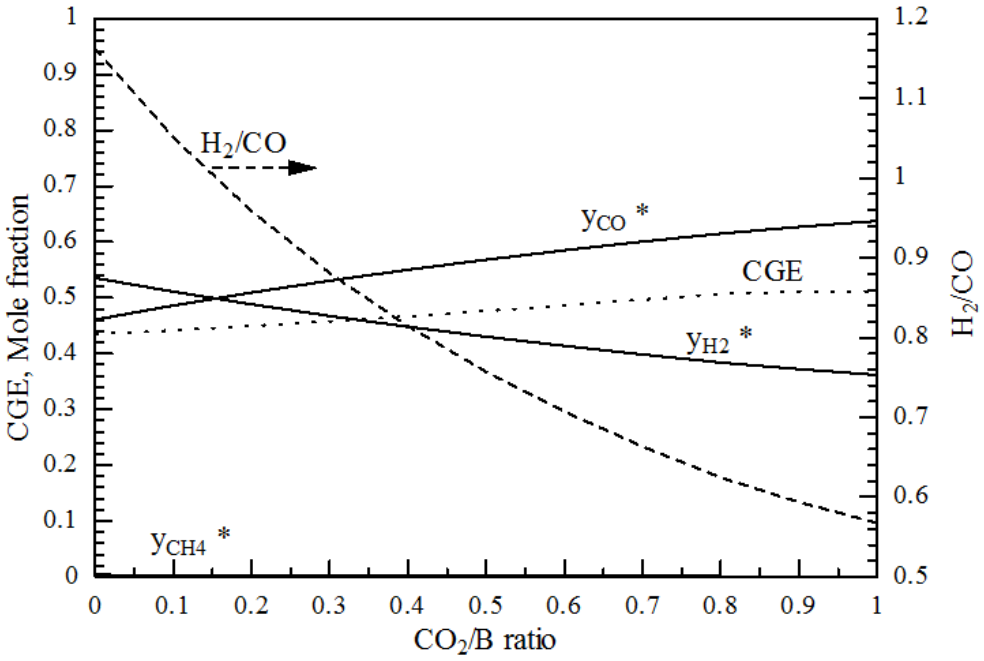

(a) Product gas compositions, CGE and H2/CO ratio Note *excluding H2O and CO2

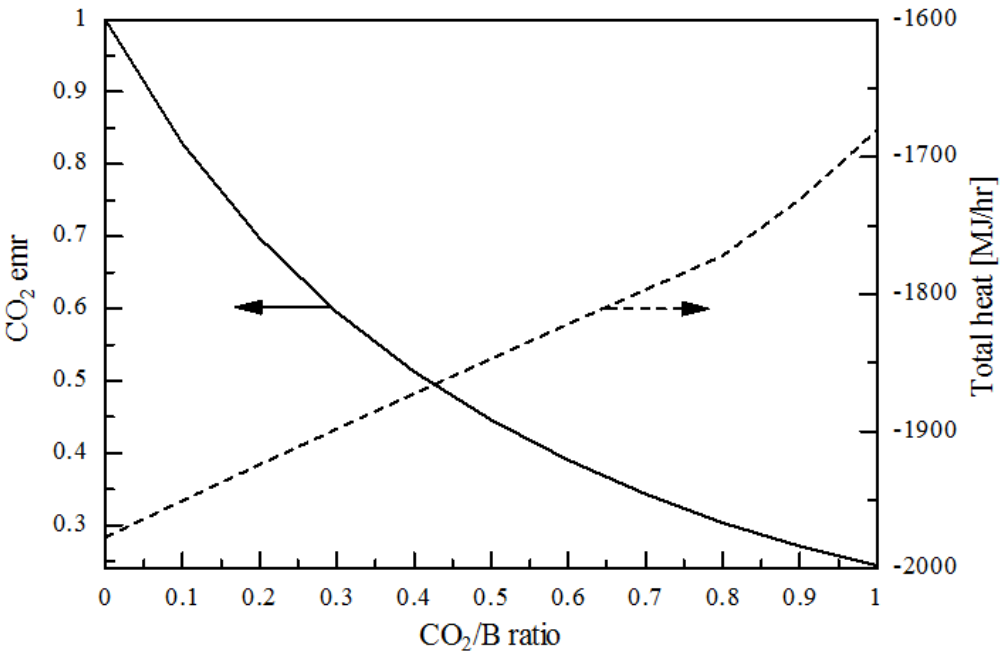

(b) CO2 emr and total heat

Figure 3.10 Effect of CO2/B feed ratio on (a) product gases and (b) CO2 emr and total heat (Tg = 600 ºC, Tr = 700 ºC, S/B = 0.4 and O2/B = 0.5)

Figure 3.10(a) shows the product gas compositions. H2 decreased with increasing CO2/B ratio but CO increased due to the same reason of the previous condition. However in this case, the composition of H2 was lower than the previous because the lower of steam for reforming with charcoal in the feed and the CO composition was higher because lower of steam caused the reverse boudouard reaction more preferred. CGE reached the maximum at CO2/B of 0.8. For CO2 emr and net heat shown in Figure 3.10(b), the lowest CO2 emr achieved was of 0.24 and the net heat obtained was 1,680 MJ/hr for CO2/B = 1. This indicates that lowering the O2/B suitable for reducing the CO2 emr while the lowering the S/B ratio is suitable for reducing the energy supplied to process.

For the best condition of each O2/B and S/B feed ratio, the next sub-part study focused on the condition at O2/B and S/B of 0.2 and 0.4, respectively. The effect of CO2/B ratio was shown in Figure 3.11.

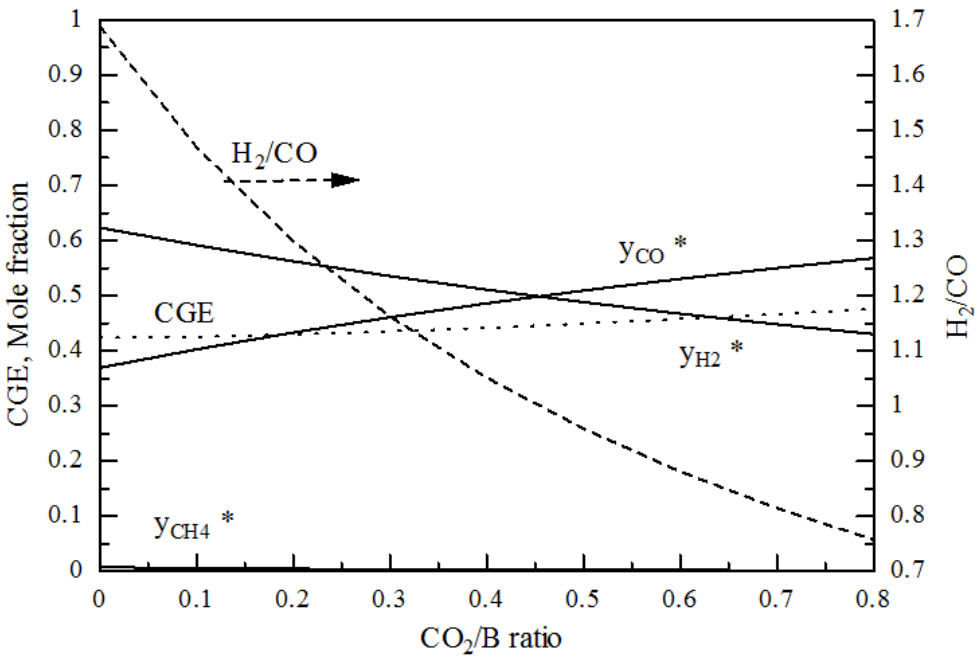

(a) Product gas compositions, CGE and H2/CO ratio Note *excluding H2O and CO2

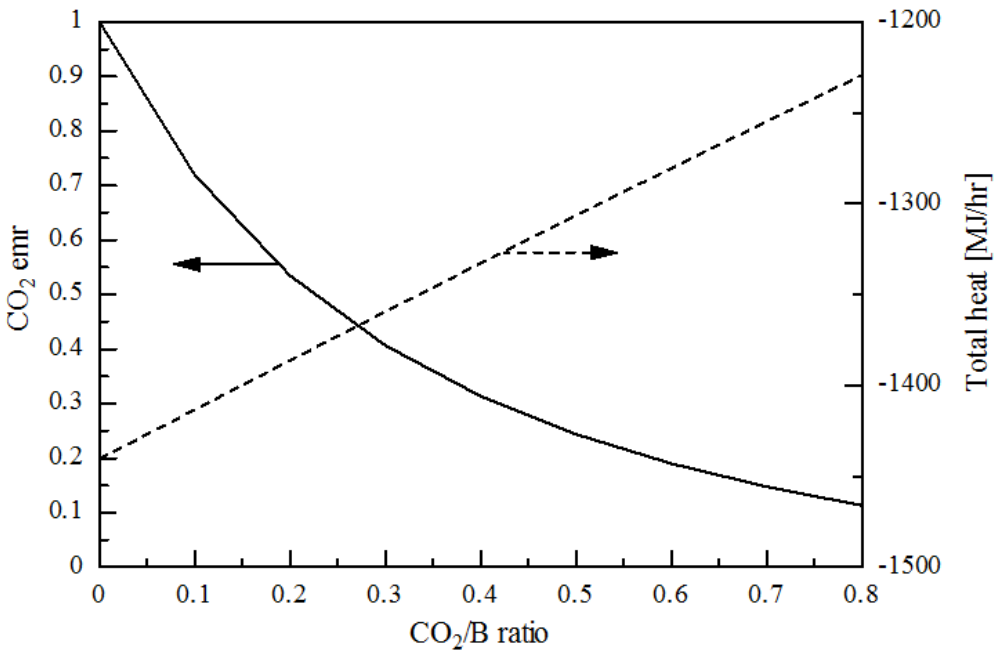

(b) CO2 emr and total heat

Figure 3.11 Effect of *CO2/B* feed ratio on (a) product gases and (b) CO2 emr and total heat (*Tg* = 600 ºC, *Tr* = 700 ºC, *S/B* = 0.4 and *O2/B* = 0.2)

In contrast, the ratio of *CO2/B* in this case reached the maximum value of 0.8 because the lack of steam and O2 from feed stream. *S/B* ratio of 0.4 and *O2/B* ratio of 0.2 are not able to produce enough CO2 for supplying to the process for the condition of *CO2/B* ratio higher than 0.8. Figure 3.11(a) shows the similar trend of product gas compositions as the previous condition, however, the CGE is lower than the previous condition because lower syngas was produced. The lack of reaction agents caused the lower yield of produced syngas. The CO2 emr shows the lowest value of 0.11 when *CO2/B* ratio is 1. Considering the net heat obtained, this condition also provides the lowest net heat of 1,229 MJ/hr because of low syngas yield.

From all of the previous conditions, the optimum condition in terms of CO2 emr, CGE and net heat obtained is proposed as *O2/B* of 0.2 and *S/B* of 0.8. The results were shown in Figure 3.12.

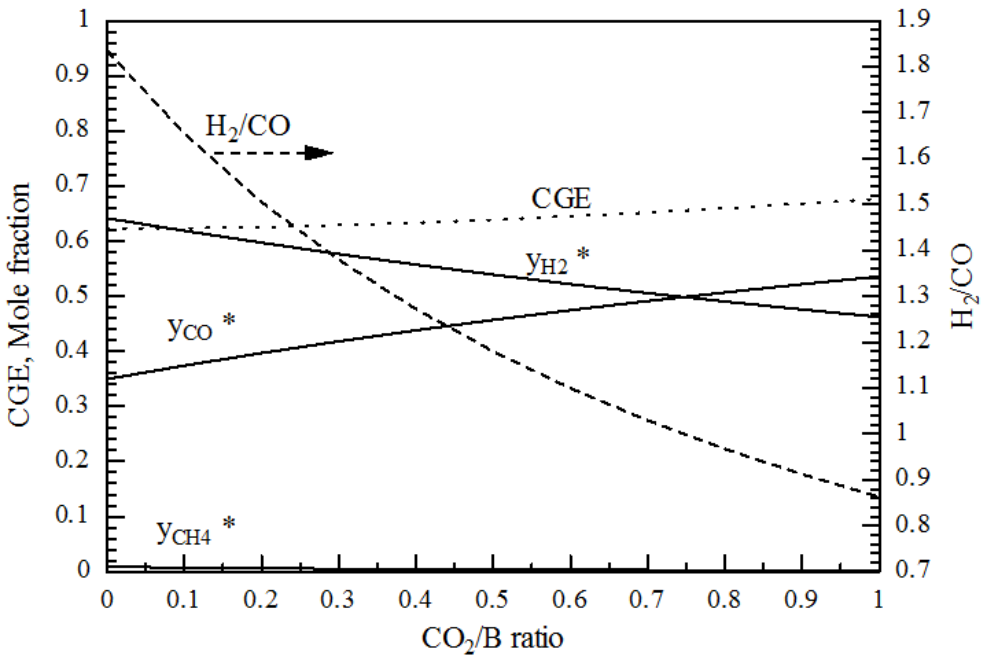

(a) Product gas compositions, CGE and H2/CO ratio Note *excluding H2O and CO2

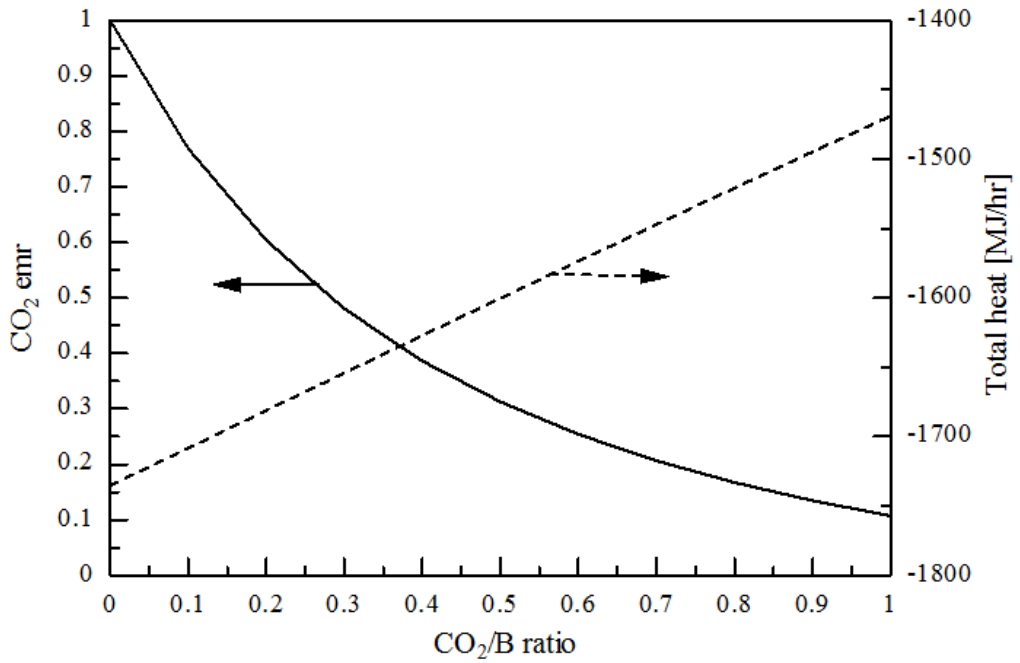

(b) CO2 emr and total heat

Figure 3.12 Effect of CO2/B feed ratio on (a) product gases and (b) CO2 emr and total heat (Tg = 600 ºC, Tr = 700 ºC, S/B = 0.8 and O2/B = 0.2)

Figure 3.12(a) shows the similar trend of gas products, but the optimum of this case acquired from the high CGE was almost equal to the case of *CO2/B* = 1, *O2/B* = 0.2 and *S/B* = 1. However, the lower *S/B* of 0.8 in this case offers lower cost in steam generation. Considering CO2 emr, this case offers the value of 0.10 (Figure 3.12(b)), which was lower than the case of *CO2/B* = 1, *O2/B* = 0.2 and *S/B* = 1. Although, the highest net heat obtained from the process, acquired from the case of *CO2/B* = 1, *O2/B* = 0.5 and *S/B* = 0.4, is 1,680 MJ/hr but CGE is 0.51 which is lower than that of the present case (*CO2/B* 1, *O2/B* 0.2 and *S/B* 0.8) of 0.67 (net heat obtained is 1,468 MJ/hr).

3.4 Reaction study of combined gasifier and reformer

This part studied the effects of temperature, %Ni loading and feed ratios on product gas compositions, carbon conversion and product gas yield.

3.4.1 Effect of temperature

In order to find out the suitable reaction temperature, tests at various reaction temperatures were conducted. Reaction temperatures of 400 ºC, 600 ºC and 800 ºC were

investigated, using only 1 g of charcoal in the quartz tube reactor with feeds of O2, CO2 and steam at a ratio of O2/CO2/S/B = 0.5/1/1/1. Product gas compositions (excluding H2O and CO2) are listed in Table 3.5 as follow.

Table 3.5 Effect of reaction temperature on product gas composition

Biomass	Reaction temperature (°C)	Time (min)	Gas composition (%mol) (excluding H_2O and CO_2)		
			H_2	CO	CH_4
Charcoal	400	30	24.64	33.26	42.09
		60	24.81	34.15	41.03
		120	43.25	56.74	-
		180	42.05	57.94	-
	600	30	43.83	56.16	n/a
		60	47.18	52.72	n/a
		120	59.20	40.80	n/a
		180	100.00	-	n/a
	800	30	12.83	87.17	n/a
		60	24.52	75.47	n/a
		120	100.00	-	n/a
		180	-	-	n/a

The results showed at reaction temperatures of 400 ºC and 600 ºC, 1 g of charcoal was not completely used after 180 minutes of reactions. However, all charcoal was reacted at reaction temperatures of 800 ºC after 120 minutes as observed by no product gas produced anymore (the actual feed ratio is *O2/CO2/S/B* = 0.33/0.66/0.66/1). The mole fractions of product gases at those operating temperatures (excluding H2O and CO2) were displayed in Figure 3.13.

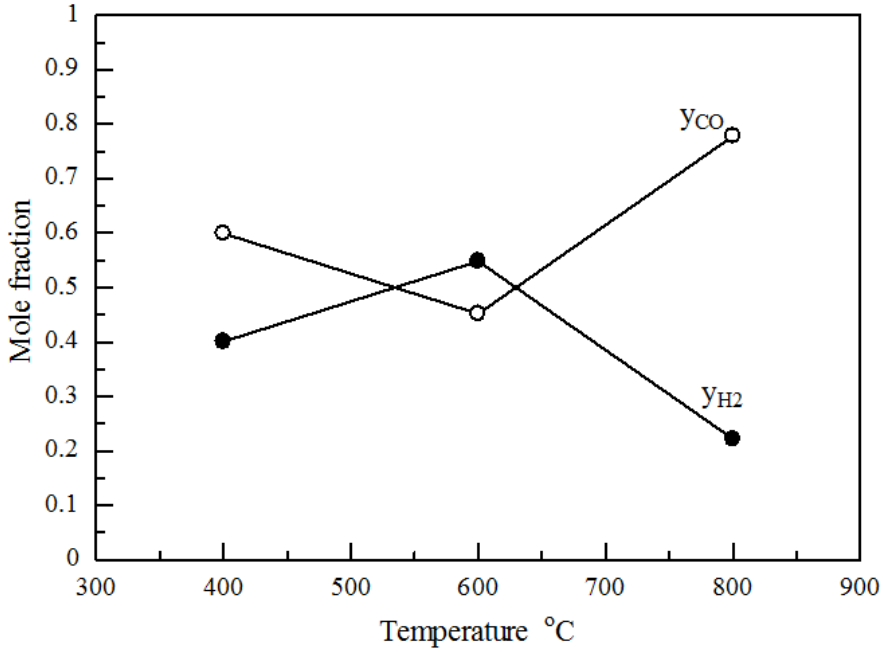

Figure 3.13 Effect of operating temperature on moles fraction of product gases, *O2/CO2/S/B* = 0.5/1/1/1 and Non-catalyst (excluding H2O and CO2)

Mole fraction of product gases at 800 ºC contained higher CO than H2, this is because reverse water gas shift and boudouard reaction are preferred at higher temperature, leading to more CO produced [53]. Carbon conversion and product gas yield were also reported in Figure 3.14.

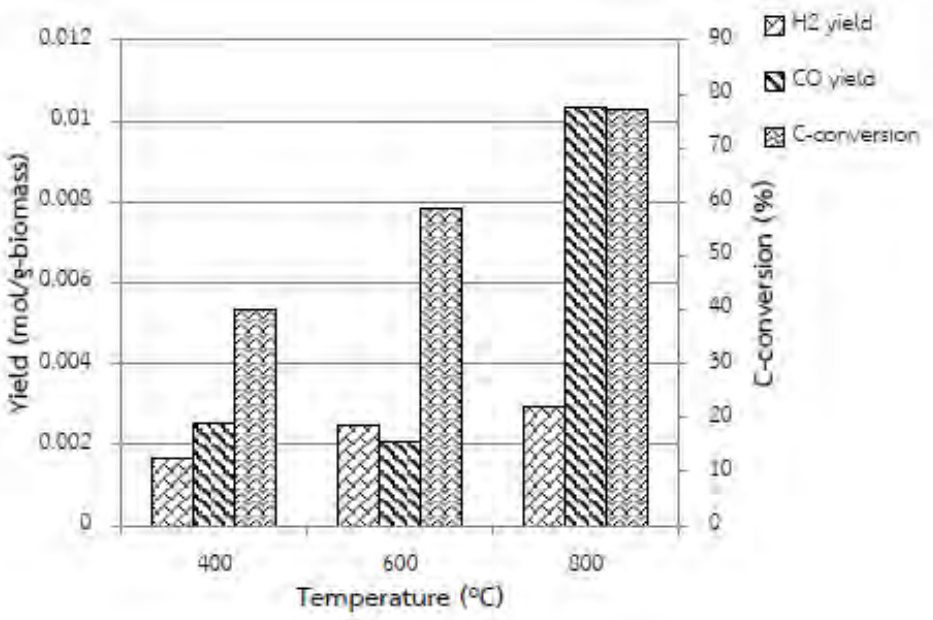

Figure 3.14 Effect of reaction temperature on carbon conversion and product gas yield, *O2/CO2/S/B* = 0.5/1/1/1 and Non-catalyst.

Carbon conversion increased with operating temperature from 40% at 400 ºC to 77% at 800 ºC. Gas yield was calculated by moles of product gas from experiment divided by gram of used biomass. Increasing reaction temperature offers more carbon conversion and product gas yield. For 800 ºC, carbon conversion reaches the maximum of 77%, moreover, H2 and CO yield also reaches the maximum.

3.4.2 Effect of Ni% loading on catalysts

From the result of the highest carbon conversion, the operating temperature of 800 ºC and *O2/CO2/S/B* feed ratio of 0.5/1/1/1 were fixed to study the effect of Ni% loading on catalysts. There values of Ni% loading of 5%Ni/SiO2, 10%Ni/SiO2 and 15%Ni/SiO2 were used for evaluating the performance of combined gasifier and reformer process. Product gas compositions are presented in Table 3.6 as follows.

Table 3.6 Effect of Ni% loading on product gas compositions

Biomass	Catalysts	Time (min)	Gas composition (%mol) (excluding H_2O and CO_2)		
			H_2	CO	CH_4
Charcoal	5%Ni/SiO_2	30	12.08	87.92	n/a
		60	22.72	77.28	n/a
		120	n/a	n/a	n/a
		180	n/a	n/a	n/a
	10%Ni/SiO_2	30	12.87	87.13	n/a
		60	23.77	76.23	n/a
		120	32.90	67.10	n/a
		180	46.38	53.62	n/a
	15%Ni/SiO_2	30	11.61	88.39	n/a
		60	16.53	83.47	n/a
		120	32.69	67.31	n/a
		180	n/a	n/a	n/a

For the cases of 10%Ni/SiO2 and 15%Ni/SiO2, 1g of charcoal was completely used. However, 5%Ni/SiO2 reached complete reaction at 100 minutes (the actual feed ratio is O2/CO2/S/B = 0.27/0.55/0.55/1).

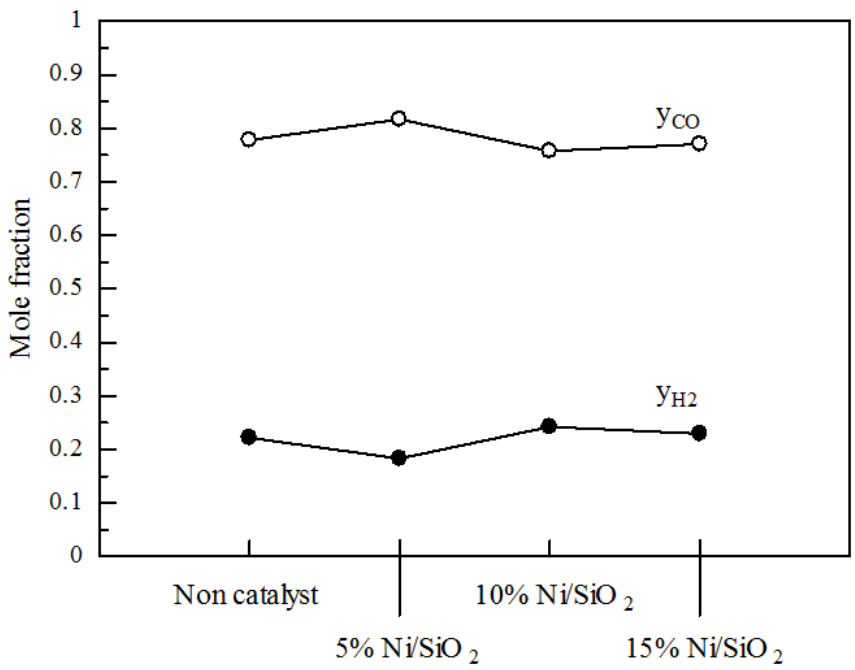

Figure 3.15 Mole fractions of product gases for catalysts with different loading, T = 800 ºC and O2/CO2/S/B = 0.5/1/1/1 (excluding H2O and CO2)

Adding the catalysts was able to improve the performance of the process by increasing H2 and CO contents. The effects of different Ni% loading were conducted for 3 hours. However, only slight changes in mole fraction of the product gases were observed (Figure 3.15) because the amount of H2 and CO increased in almost proportional ratio.

Therefore, adding reforming catalysts in the reactor could improve the performance by upgrading syngas product as observed in increasing of product gas yield with higher Ni% loading (Figure -.16). Then, carbon conversion was also investigated and the results were displayed in Figure 3.16.

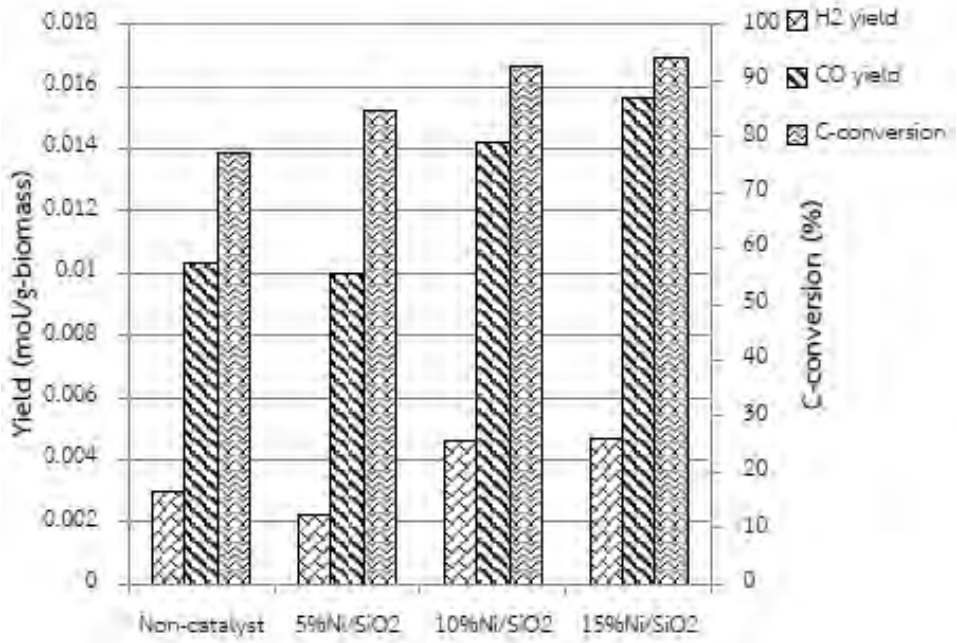

Figure 3.16 Carbon conversions of various catalysts, T = 800 ºC and O2/CO2/S/B = 0.5/1/1/1

Carbon to gas conversion was calculated by total moles of carbon atom in gas product divided by moles of 1 g charcoal. So, increasing in carbon conversion is due to increase of CO in syngas product as presented in Figure 3.16. By the reason in quantity of syngas product compared to percentage of Ni loading and carbon conversion, so the optimum catalyst is 10%Ni/SiO2.

Then, the further studied using 10%Ni/SiO2 catalyst and operating temperature of 800 ºC were conducted. The results of the effects of O2/B, S/B and CO2/B were described as follows.

3.4.3 Effect of O2/B feed ratio

The presence of O2 in feed stream offers both advantage and disadvantage. On one hand, higher O2 causes the reaction preferably to combustion from partial oxidation reaction which means that more CO2 was produced than CO. On the other hand, introducing O2 can be reduced heat supplying to the reactor due to the exothermic of combustion reaction [35]. Figure 3.17 shows the total moles of product gas, represented product gas yield, after 3 hours of reaction time, introducing O2 from ratio 0 to 0.5 could slightly improve the CO via partial oxidation reaction. Product gas composition with time on stream is shown in Table 3.7.

Table 3.7 Effect of O2/B feed ratio on product gas composition

Biomass	O_2/B ratio	Time (min)	Gas composition (%mol) (excluding H_2O and CO_2)		
			H_2	CO	CH_4
Charcoal	0	30	14.50	85.50	n/a
		60	24.33	75.67	n/a
		120	31.07	68.93	n/a
		180	33.05	66.95	n/a
	0.5	30	12.87	87.13	n/a
		60	23.77	76.23	n/a
		120	32.90	67.10	n/a
		180	46.38	53.62	n/a

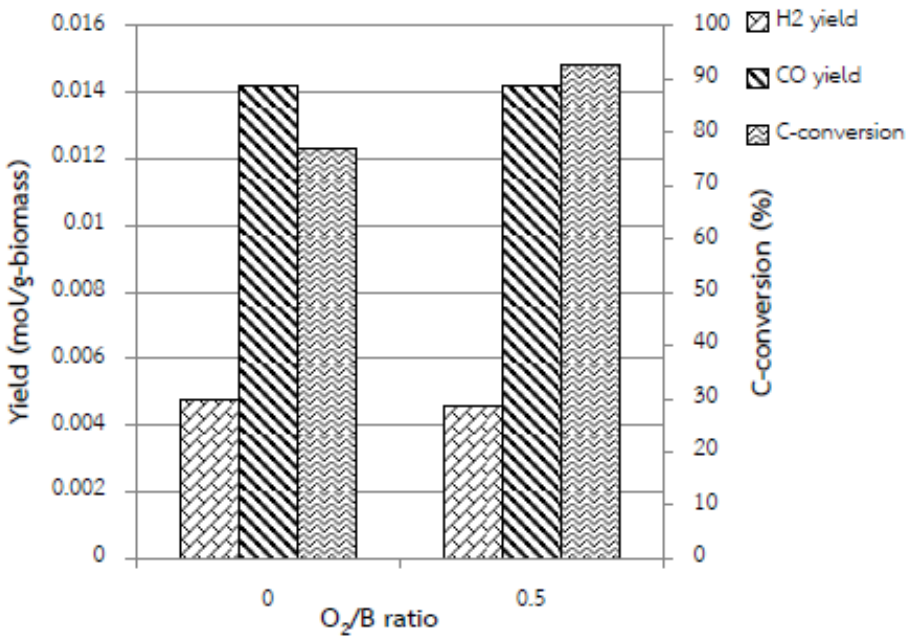

Figure 3.17 Effect of O2/B ratio on carbon conversions and product gas yield, T = 800 ºC, CO2/S/B = 1/1/1 and used 10%Ni/SiO2

Introducing the O2 can improve the process performance as observed in Figure 3.17, by increasing O2/B ratio from 0 to 0.5 increased the carbon conversion by 17%.

3.4.4 Effect of S/B ratio

The effect of S/B feed ratio was also investigated in the experimental studies. S/B feed ratios were varied by 0, 1 and 2. All the results indicated that 1 g of charcoal was completely used in 3 hours reaction time. The product gas composition is listed in Table 3.9 as below.

Table 3.8 Effect of S/B feed ratio on product gas composition

Biomass	S/B	Time (min)	Gas composition (%mol) (excluding H_2O and CO_2)		
			H_2	CO	CH_4
Charcoal	0	30	13.20	86.80	n/a
		60	15.42	84.58	n/a
		120	20.28	79.72	n/a
		180	100.00	-	n/a
	1	30	12.87	87.13	n/a
		60	23.77	76.23	n/a
		120	32.90	67.10	n/a
		180	46.38	53.62	n/a
	2	30	14.67	85.33	n/a
		60	39.22	60.78	n/a
		120	50.91	49.09	n/a
		180	-	-	n/a

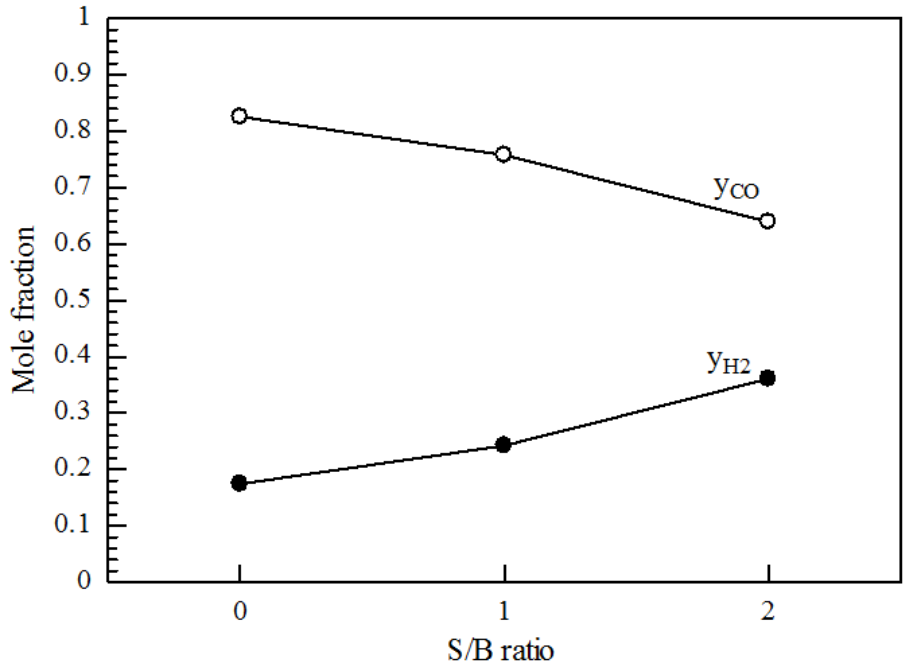

Figure 3.18 Effect of S/B feed ratio on mole fraction of product gases, T = 800 ºC, O2/CO2/B = 0.5/1/1 and used 10%Ni/SiO2 (excluding H2O and CO2)

Figure 3.18 shows the effect of S/B ratio on product gas mole fractions. This can be observed that higher S/B ratio offers higher mole fraction of H2 because more steam shifts the

steam reforming [15] and water gas shift reaction also plays an important role in decreasing of CO [10], according to the product gas yield (Figure 3.19).

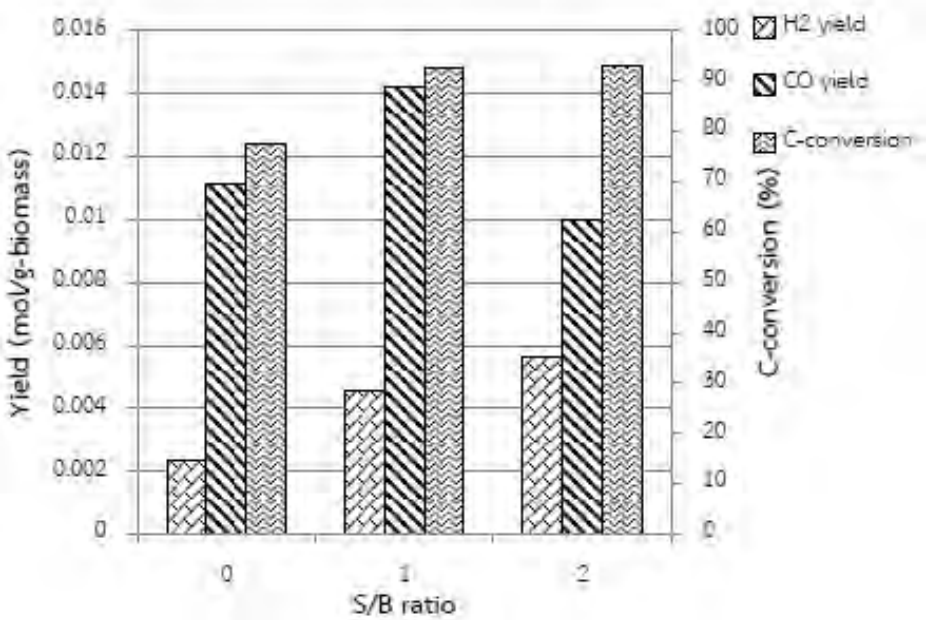

Figure 3.19 Effect of S/B feed ratio on carbon conversion and product gas yield, T = 800 ºC, O2/CO2/B = 0.5/1/1 and used 10%Ni/SiO2

Figure 3.19 shows that the carbon conversion increased from 77% to 94% by increasing S/B ratio from 0 to 2. However, the product gas yield of H2 increased from S/B ratio 0 to 2 due to water gas shift reaction [10]. But, CO yield was observed for the maximum at S/B ratio of 1. In overview, in this case of the experimental studies shows poor performance in syngas production due to presence of CO2 in the feed stream compared to other research with no CO2 in feed stream [10].

3.4.5 Effect of CO2/B feed ratio

The effect of CO2/B ratio is another interesting parameter. The higher CO2/B ratio indicated the case with more CO2 recycled back to the process. This offers an advantage in utilizing CO2 instead of emitting it to atmosphere. Results of product gas composition are shown in Table 3.9 as below.

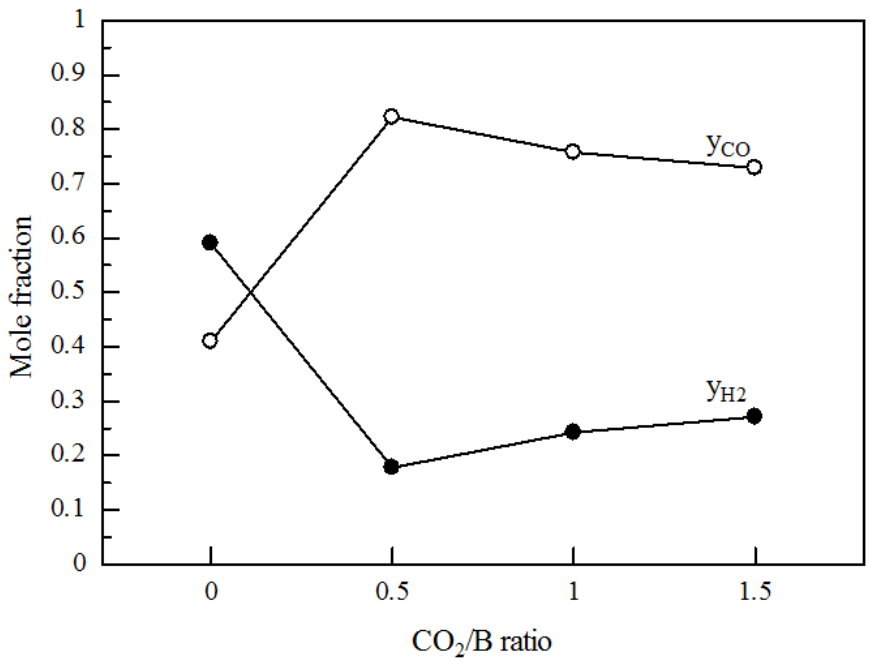

Figure 3.20 Effect of CO2/B feed ratio on mole fraction of product gases on, T = 800 ºC, O2/S/B = 0.5/1/1 and used 10%Ni/SiO2 (excluding H2O and CO2)

Table 3.9 Effect of CO2/B feed ratio on product gas composition

Biomass	CO_2/B ratio	Time (min)	Gas composition (%mol) (excluding H_2O and CO_2)		
			H_2	CO	CH_4
Charcoal	0	30	38.01	61.99	n/a
		60	59.84	40.16	n/a
		120	59.22	40.78	n/a
		180	66.28	33.72	n/a
	0.5	30	14.67	85.33	n/a
		60	16.74	83.26	n/a
		120	20.96	79.04	n/a
		180	29.17	70.83	n/a

Table 3.9 Effect of CO2/B feed ratio on product gas composition (cont'd)

Biomass	CO_2/B ratio	Time (min)	Gas composition (%mol) (excluding H_2O and CO_2)		
			H_2	CO	CH_4
Charcoal	1	30	12.87	87.13	n/a
		60	23.77	76.23	n/a
		120	32.90	67.10	n/a
		180	46.38	53.62	n/a
	1.5	30	18.28	81.72	n/a
		60	25.56	74.44	n/a
		120	33.08	66.92	n/a
		180	34.78	65.22	n/a

According to the previous work of Wang et al. [15] on the effect of CO2 to propane molar feed ratio, the results indicated that moles of H2 in product gas were close in both cases of CO2 to propane molar ratio 1 and 3. The results from this study, as shown in Figure 3.20, show the similar trend.

For CO2/B ratio of 0, this can represented the main reaction consisting of steam and partial oxidation. This offered the highest H2 in syngas product and also high CO. But in term of CO2 emission, this offers the low performance. The suitable ratio was CO2/B = 1 due to the highest moles of H2 and CO in product gas. Carbon conversion and product gas yield were also investigated as presented in Figure 3.21.

And Figure 3.21 also reported that product gas yield for the case of CO2/B ratio of 0 shows the highest but dropped with the addition of CO2 in the feed stream. The highest carbon conversion was observed in the case of CO2/B ratio 1; this can be inferred that charcoal was converted into syngas product.

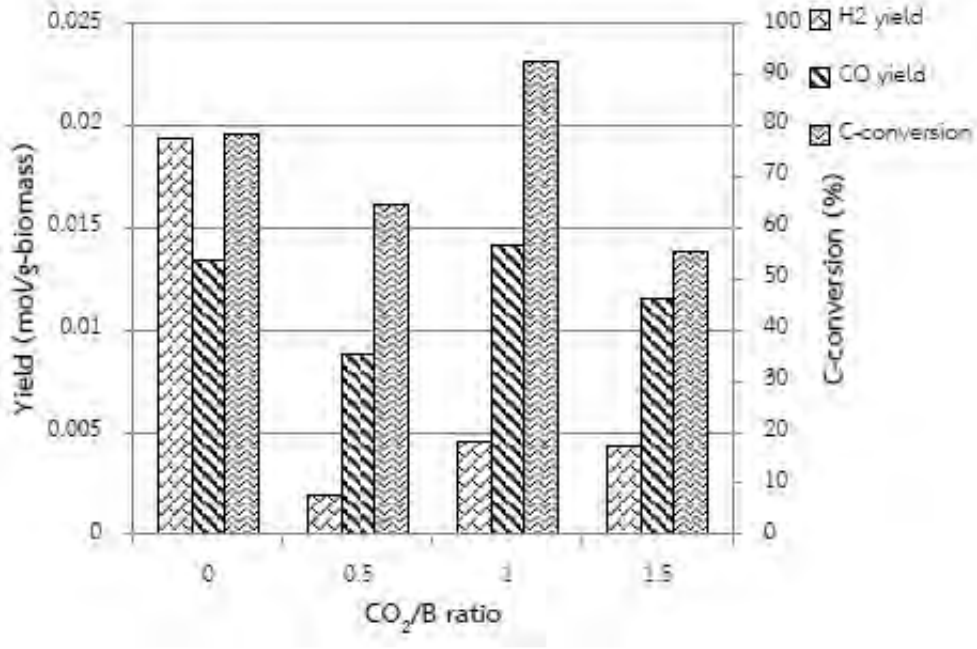

Figure 3.21 Effect of CO2/B feed ratio on carbon conversion and product gas yield, T = 800 ºC, O2/S/B = 0.5/1/1 and used 10%Ni/SiO2

Table 3.11 Syngas ratio on various feed ratio

Conditions	H_2/CO
$O_2/S/CO_2/B$ = 0.5/1/1/1	0.32
$O_2/S/CO_2/B$ = 0/1/1/1	0.34
$O_2/S/CO_2/B$ = 0.5/0/1/1	0.21
$O_2/S/CO_2/B$ = 0.5/2/1/1	0.56
$O_2/S/CO_2/B$ = 0.5/1/0/1	1.44
$O_2/S/CO_2/B$ = 0.5/1/0.5/1	0.22
$O_2/S/CO_2/B$ = 0.5/1/1.5/1	0.37

Finally, Syngas ratio was also observed in all of studied cases. Table 3.11 shows that syngas ratio from various O2/B was not much different. By increasing S/B ratio, syngas ratio becomes higher. When increasing CO2/B ratio, syngas ratio can be adjusted in wider range than being adjusted by steam and O2 (0.2-1.4).

3.5 Comparison of model and experimental

For case of reaction temperature 800 ºC, the mole fraction of product gas from experimental was calculation using raw data as shown in Figure 3.22. Comparison of product gas mole fraction on different percentage from modeling and experimental was conducted to investigate the different of modeling and experimental.

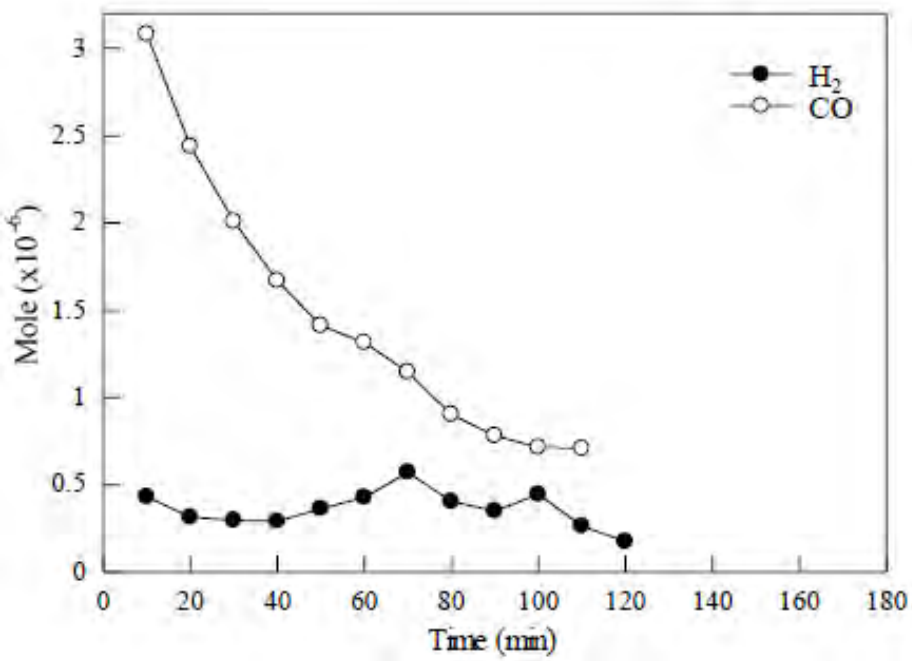

Figure 3.22 Raw result of product gas from experiment (T = 800 ºC, non-catalyst and O2/S/CO2/B = 0.5/1/1/1)

For experimental, the product gas mole fraction was calculated as yH2 = 0.222 and yCO = 0.778, for modeling, yH2 = 0.434 and yCO = 0.566. Then calculate the different percentage between modeling and experimental of H2 was 48.85% and CO was 37.45%.

4 CONCLUSIONS AND RECOMMENDATIONS

In this work, the performance of combined gasifier and reformer using charcoal was evaluated on product gas composition, CO_2 emr, CGE, carbon conversion, product gas yield and H_2/CO ratio. The effects of temperature, feed ratio and Ni% loading on catalyst were considered. The conclusions and recommendations for future work were listed below.

4.1 Conclusions

1. The thermodynamic analysis results indicated that the suitable operating temperature was 700 ºC because this temperature offered the highest CGE and optimum net heat obtained from process. The suitable O_2/B and S/B feed ratios were at 0.2 and 0.4, respectively, which are considered in terms of CGE and net heat obtained. Increasing CO_2/B ratio decreased the CO_2 emr, but lower net heat and H_2 content in syngas product were also obtained. H_2/CO ratio was easier adjusted by altering the CO_2/B in the feed stream.

2. The results of the experimental study showed the good agreement with thermodynamic analysis simulation. This can be observed from the trend of the results. Higher operating temperature leaded to more carbon conversion and syngas product. Results of O_2/B feed ratio deviated slightly from simulation results. The H_2 content in syngas product increased with increasing S/B ratio. The higher CO_2/B feed ratio offered increasing of CO and decreased H_2. Moreover, the H_2/CO ratio can be adjusted from 0.2 to 1.4 by varying the CO_2/B feed ratio.

3. Catalyst characterization revealed that higher Ni% loading on SiO_2 caused reduction in surface area of catalyst as observed by BET method. From the results of H_2-TPR peaks, the suitable reducing temperature was in range of 350 ºC – 400 ºC. 10% Ni/SiO_2 was the optimum catalyst according to the suitable syngas product.

4.2 Recommendation

1. From the reaction studied, using the mass flow controller offered the higher accurate in adjusting flow rate than using the needle valve.

2. Gas chromatography should examine the light hydrocarbons, this offers higher accurate in calculating carbon conversion.

3. The size of quartz tube reactor affects the height of charcoal pack bed, bigger quartz tube reactor offers the shorter pack bed, leading to reduce error in temperature profile of furnace.

4. The effect of catalyst support should be considered.

5. Split furnace to two units can be improved in controlling temperature profile of reactor.

5 REFERENCES

[1] McKendry, P. Energy production from biomass (part 1) overview of biomass. Bioresource Technology 83 (2002): 37-46.

[2] Cocco, D., Serra, F., and Tola, V. Assessment of energy and economic benefits arising from syngas storage in IGCC power plants. Energy 58 (2013): 635-643.

[3] Sorgenfrei, M. and Tsatsaronis, G. Design and evaluation of an IGCC power plant using iron-based syngas chemical-looping (SCL) combustion. Applied Energy 113 (2014): 1958-1964.

[4] Khine, M.S.S., Chen, L., Zhang, S., Lin, J., and Jiang, S.P. Syngas production by catalytic partial oxidation of methane over (La0.7A0.3)BO3 (A = Ba, Ca, Mg, Sr, and B = Cr or Fe) perovskite oxides for portable fuel cell applications. International Journal of Hydrogen Energy 38(30) (2013): 13300-13308.

[5] Hackett, G.A., et al. Performance of solid oxide fuel cells operated with coal syngas provided directly from a gasification process. Journal of Power Sources 214 (2012): 142-152.

[6] Mondal, P., Dang, G.S., and Garg, M.O. Syngas production through gasification and cleanup for downstream applications — Recent developments. Fuel Processing Technology 92(8) (2011): 1395-1410.

[7] H.C., B. and M.J., C. CO2 as a Carbon Neutral Fuel Source via Enhanced Biomass Gasification. Environment Science Technology 43 (2009): 9030-9037.

[8] Cheng, G., et al. Gasification of biomass micron fuel with oxygen-enriched air: Thermogravimetric analysis and gasification in a cyclone furnace. Energy 43(1) (2012): 329-333.

[9] Moghtaderi, B. Effects of controlling parameters on production of hydrogen by catalytic steam gasification of biomass at low temperatures. Fuel 86(15) (2007): 2422-2430.

[10] Wei, L., Xu, S., Zhang, L., Liu, C., Zhu, H., and Liu, S. Steam gasification of biomass for hydrogen-rich gas in a free-fall reactor. International Journal of Hydrogen Energy 32(1) (2007): 24-31.

[11] Chaiwatanodom, P., Vivanpatarakij, S., and Assabumrungrat, S. Thermodynamic analysis of biomass gasification with CO2 recycle for synthesis gas production. Applied Energy 114 (2014): 10-17.

[12] Renganathan, T., Yadav, M.V., Pushpavanam, S., Voolapalli, R.K., and Cho, Y.S. CO2 utilization for gasification of carbonaceous feedstocks: A thermodynamic analysis. Chemical Engineering Science 83 (2012): 159-170.

[13] Antzara, A., Heracleous, E., Bukur, D.B., and Lemonidou, A.A. Thermodynamic analysis of hydrogen production via chemical looping steam methane reforming coupled with in situ CO2 capture. International Journal of Greenhouse Gas Control 32 (2015): 115-128.

[14] Tomishige, K., Asadullah, M., and Kunimori, K. Syngas production by biomass gasification using Rh/CeO2/SiO2 catalysts and fluidized bed reactor. Catalysis Today 89(4) (2004): 389-403.

[15] Wang, X., Wang, N., Zhao, J., and Wang, L. Thermodynamic analysis of propane dry and steam reforming for synthesis gas or hydrogen production. International Journal of Hydrogen Energy 35(23) (2010): 12800-12807.

[16] Pompeo, F., Nichio, N.N., Souza, M.M.V.M., Cesar, D.V., Ferretti, O.A., and Schmal, M. Study of Ni and Pt catalysts supported on α-Al2O3 and ZrO2 applied in methane reforming with CO2. Applied Catalysis A: General 316(2) (2007): 175-183.

[17] Liu, D., Quek, X.-Y., Wah, H.H.A., Zeng, G., Li, Y., and Yang, Y. Carbon dioxide reforming of methane over nickel-grafted SBA-15 and MCM-41 catalysts. Catalysis Today 148(3-4) (2009): 243-250.

[18] Horváth, A., et al. Sol-derived AuNi/MgAl2O4 catalysts: Formation, structure and activity in dry reforming of methane. Applied Catalysis A: General 468 (2013): 250-259.

[19] Taufiq-Yap, Y.H., Sudarno, Rashid, U., and Zainal, Z. CeO2–SiO2 supported nickel catalysts for dry reforming of methane toward syngas production. Applied Catalysis A: General 468 (2013): 359-369.

[20] Huang, B.-S., Chen, H.-Y., Chuang, K.-H., Yang, R.-X., and Wey, M.-Y. Hydrogen production by biomass gasification in a fluidized-bed reactor promoted by an Fe/CaO catalyst. International Journal of Hydrogen Energy 37(8) (2012): 6511-6518.

[21] Bermúdez, J.M., Fidalgo, B., Arenillas, A., and Menéndez, J.A. CO2 reforming of coke oven gas over a Ni/γAl2O3 catalyst to produce syngas for methanol synthesis. Fuel 94 (2012): 197-203.

[22] Fakeeha, A.H., Khan, W.U., Al-Fatesh, A.S., and Abasaeed, A.E. Stabilities of zeolite-supported Ni catalysts for dry reforming of methane. Chinese Journal of Catalysis 34(4) (2013): 764-768.

[23] Gao, N., Li, A., Quan, C., and Gao, F. Hydrogen-rich gas production from biomass steam gasification in an updraft fixed-bed gasifier combined with a porous ceramic reformer. International Journal of Hydrogen Energy 33(20) (2008): 5430-5438.

[24] Wu, C. and Williams, P.T. Hydrogen production by steam gasification of polypropylene with various nickel catalysts. Applied Catalysis B: Environmental 87(3-4) (2009): 152-161.

[25] Wu, C., Wang, Z., Huang, J., and Williams, P.T. Pyrolysis/gasification of cellulose, hemicellulose and lignin for hydrogen production in the presence of various nickel-based catalysts. Fuel 106 (2013): 697-706.

[26] Puig-Arnavat, M., Bruno, J.C., and Coronas, A. Review and analysis of biomass gasification models. Renewable and Sustainable Energy Reviews 14(9) (2010): 2841-2851.

[27] Gujar, A.C., Baik, J., Garceau, N., Muradov, N., and T-Raissi, A. Oxygen-blown gasification of pine charcoal in a top-lit downdraft moving-hearth gasifier. Fuel 118 (2014): 27-32.

[28] Rajvanshi, A.K. Biomass Gasification. Alternative Energy in Agriculture. Vol. II. India: CRC Press, 1986.

[29] Schapfer, P. and Tobler, J. Theoretical and Practical Investigations Upon the Driving of Motor Vehicles with Wood Gas. 1937.

[30] Rostrup-Nielsen, J.R. and Hansen, J.B. Steam Reforming for Fuel Cells. (2011): 49-71.

[31] Smith, M.W. and Shekhawat, D. Catalytic Partial Oxidation. (2011): 73-128.

[32] Gao, J., Hou, Z., Lou, H., and Zheng, X. Dry (CO2) Reforming. (2011): 191-221.

[33] Peters, L., Hussain, A., Follmann, M., Melin, T., and Hägg, M.B. CO2 removal from natural gas by employing amine absorption and membrane technology—A technical and economical analysis. Chemical Engineering Journal 172(2-3) (2011): 952-960.

[34] Udomsirichakorn, J. and Salam, P.A. Review of hydrogen-enriched gas production from steam gasification of biomass: The prospect of CaO-based chemical looping gasification. Renewable and Sustainable Energy Reviews 30 (2014): 565-579.

[35] Lv, P.M., Xiong, Z.H., Chang, J., Wu, C.Z., Chen, Y., and Zhu, J.X. An experimental study on biomass air-steam gasification in a fluidized bed. Bioresour Technol 95(1) (2004): 95-101.

[36] Zhang, R., Cummer, K., Suby, A., and Brown, R.C. Biomass-derived hydrogen from an air-blown gasifier. Fuel Processing Technology 86(8) (2005): 861-874.

[37] Song, T., Wu, J., Shen, L., and Xiao, J. Experimental investigation on hydrogen production from biomass gasification in interconnected fluidized beds. Biomass and Bioenergy 36 (2012): 258-267.

[38] Ahmed, I. and Gupta, A.K. Characteristics of cardboard and paper gasification with CO2. Applied Energy 86(12) (2009): 2626-2634.

[39] Garcia, L., Salvador, M.L., Arauzo, J., and Bilbao, R. CO2 as a gasifying agent for gas production from 2 pine sawdust at low temperatures using a Ni-Al coprecipitated catalyst. Fuel Processing Technology 69 (2001): 157-174.

[40] Karim, G.A. and M.M., M. A kinetic investigation of the reforming of natural gas for the production of hydrogen. Hydrogen Energy 5 (1979): 293-304.

[41] Park, H.J., et al. Steam reforming of biomass gasification tar using benzene as a model compound over various Ni supported metal oxide catalysts. Bioresource Technology 101 Suppl 1 (2010): S101-3.

[42] Fierro, V., Klouz, V., Akdim, O., and Mirodatos, C. Oxidative reforming of biomass derived ethanol for hydrogen production in fuel cell applications. Catalysis Today 75 (2002): 141-144.

[43] Vicente, J., Ereña, J., Montero, C., Azkoiti, M.J., Bilbao, J., and Gayubo, A.G. Reaction pathway for ethanol steam reforming on a Ni/SiO2 catalyst including coke formation. International Journal of Hydrogen Energy 39(33) (2014): 18820-18834.

[44] Bermúdez, J.M., Fidalgo, B., Arenillas, A., and Menéndez, J.A. Dry reforming of coke oven gases over activated carbon to produce syngas for methanol synthesis. Fuel 89(10) (2010): 2897-2902.

[45] Zhang, J. and Li, F. Coke-resistant Ni@SiO2 catalyst for dry reforming of methane. Applied Catalysis B: Environmental 176-177 (2015): 513-521.

[46] Li, B., Xu, X., and Zhang, S. Synthesis gas production in the combined CO2 reforming with partial oxidation of methane over Ce-promoted Ni/SiO2 catalysts. International Journal of Hydrogen Energy 38(2) (2013): 890-900.

[47] Rulerk, D., Assabumrungrat, S., and Vivanpatarakij, S. Removal of tar from biomass gasification process by steam reforming over nickel catalysts. Master of Engineering, Chemical Engineering Chulalongkorn University, 2011.

[48] Rodrigues, R., Secchi, A.R., Marcílio, N.R., and Godinho, M. Modeling of biomass gasification applied to a combined gasifier- combustor unit equilibrium and kinetic approaches. 10th International Symposium on Process Systems Engineering (2009).

[49] Channiwala, S.A. and Parikh, P.P. A unified correlation for estimating HHV of solid liqiud and gaseous fuels. Fuel 81 (2002): 1051-1063.

[50] Ghassemi, H. and Shahsavan-Markadeh, R. Effects of various operational parameters on biomass gasification process; a modified equilibrium model. Energy Conversion and Management 79 (2014): 18-24.

[51] Wang, Y., Wu, R., and Zhao, Y. Effect of ZrO2 promoter on structure and catalytic activity of the Ni/SiO2 catalyst for CO methanation in hydrogen-rich gases. Catalysis Today 158(3-4) (2010): 470-474.

[52] Gopaul, S.G. and Dutta, A. Dry reforming of multiple biogas types for syngas production simulated using Aspen Plus: The use of partial oxidation and hydrogen combustion to achieve thermo-neutrality. International Journal of Hydrogen Energy 40(19) (2015): 6307-6318.

[53] Franco, C., Pinto, F., Gulyurtlu, I., and Cabrita, I. The study of reactions influencing the biomass steam gasification process. Fuel 82 (2003): 835-842.

[54] Smith, J.M., Van Ness, H.C., and Abbott, M.M. Introduction to Chemical Engineering Thermodynamics, ed. 7th. McGraw-Hill Science

Output

- Paripat Kraisornkachit, Supawat Vivanpatarakij, Suksun Amornraksa, Lida Simasatitkul, Suttichai Assabumrungrat. Performance evaluation of different combined systems of biochar gasifier, reformer and CO2 capture unit for synthesis gas production. International Journal of Hydrogen Energy 41 (2016):13408-13418.

Appendix

INTERNATIONAL JOURNAL OF HYDROGEN ENERGY 41 (2016) 13408–13418

Available online at www.sciencedirect.com

ScienceDirect

journal homepage: www.elsevier.com/locate/he

Performance evaluation of different combined systems of biochar gasifier, reformer and CO_2 capture unit for synthesis gas production

Paripat Kraisornkachit [a], *Supawat Vivanpatarakij* [b,*], *Suksun Amornraksa* [c], *Lida Simasatitkul* [d], *Suttichai Assabumrungrat* [a]

[a] *Center of Excellence in Catalysis and Catalytic Reaction Engineering, Department of Chemical Engineering, Faculty of Engineering, Chulalongkorn University, Phyathai Road, Wang Mai, Phatumwan, Bangkok 10330, Thailand*

[b] *Energy Research Institute, Chulalongkorn University, Phyathai Road, Wang Mai, Phatumwan, Bangkok 10330, Thailand*

[c] *The Sirindhorn International Thai-German Graduate School of Engineering (TGGS), King Mongkut's University of Technology North Bangkok, Pracharat 1 Road, Wongsawang, Bangsue, Bangkok, Thailand*

[d] *Department of Industrial Chemistry, King Mongkut's University of Technology North Bangkok, Pracharat 1 Road, Wongsawang, Bangsue, Bangkok, Thailand*

ARTICLE INFO

Article history:
Received 3 March 2016
Received in revised form
31 May 2016
Accepted 4 June 2016
Available online 21 June 2016

Keywords:
Biochar gasification
CO_2 reforming
Synthesis gas production

ABSTRACT

The performance of different combined systems of biochar gasifier and reformer, with and without CO_2 recycle, was evaluated and compared in terms of cold gas efficiency (CGE), hydrogen content in syngas product, gasification system efficiency (GSE), total net heat, and CO_2 emission ratio (CO_2 EMR). Effects of various operating parameters such as feed ratio and operating temperature were investigated. The biochar, represented by mangrove tree charcoal, steam, O_2 and CO_2 were used to produce syngas product. The results revealed that the performance of the conventional systems were inferior to the ones with reformer. Increasing operating temperature offered higher CGE and could reduce CO_2 EMR. Amount of CO_2 EMR was increased with an increase in O_2/C feed ratio but it was an opposite direction at O_2/C feed ratio higher than 0.2. Higher S/C feed ratio offered higher H_2 content in the syngas product with the limitation of S/C at 1.2. The use of CO_2 in the feed produced the syngas product with lower H_2/CO. The combined gasifier and reformer with Pre-CO_2 recycle (*CBGR-Pre-reCO_2*) was the most suitable process to produce syngas with high CGE while the combined gasifier and reformer with Post-CO_2 recycle (*CBGR-Post-reCO_2*) produced syngas with low H_2/CO.

Introduction

Hydrogen has recently gained much interest as an alternative energy source, because of its high heating value and environmentally friendly nature. Synthesis gas (syngas), consisting of hydrogen and carbon monoxide, can be produced by using biomass or hydrocarbons as feedstocks. Syngas applications can be used in fuel cell [1,2] and various downstream processes [3,4]. Additionally, biomass offers

* *Corresponding author.*
E-mail address: supawat.v@chula.ac.th (S. Vivanpatarakij).

http://dx.doi.org/10.1016/j.ijhydene.2016.06.021
0360-3199/

more advantage than the hydrocarbons as it causes less greenhouse gases emission [5]. Gasification is a well-known applied technology and proven process for converting biomass into syngas due to the high efficiency. Zhang et al. [6] investigated the H_2 production from wet biomass steam gasification using CaO/MgO as catalyst. The optimal condition where H_2 content is high and CO_2 content is low was found at operating temperature between 500 and 600 °C and steam/biomass feed ratio in range of 0.5–1. Supercritical water gasification of biomass was recently reviewed by Reddy et al. [7]. In general, the H_2 yield can be increased by increasing the reaction temperature. Various types of utilizer (gasifying agent) can be used as raw material in the gasification process. Air is commonly used as a gasifying agent due to the availability and low cost, but it offers low quality of syngas because of nitrogen impurity [8]. Using pure oxygen as a gasifying agent can offer higher syngas quality but it contributes to very high operating cost [9]. Using steam as a gasifying agent can provide more hydrogen yield. However, high energy consumption is required as a result of high operating temperature [10,11]. Wei et al. [11] studied the biomass gasification using steam and reported that the presence of steam increased the H_2 gas yield. Moreover, residue char and tar were reduced with higher steam/biomass feed ratio. CO_2 has recently been proposed for use as a gasifying agent because of several advantages. The use of CO_2 offers less CO_2 emission, producing more reactive char and beneficial in adjusting syngas ratio [12,13]. It has been reported that using CO_2 as a gasifying agent provided lower reaction rates than using steam [14].

Undesirable heavy-hydrocarbon compounds (tar) are also produced from gasification process [15]. To overcome such a difficulty, reforming process of hydrocarbon by using steam or CO_2 can be used in order to reduce tar and produce more syngas product [15]. It has been reported that steam reforming produces higher H_2 content in syngas product and also offers the benefit of coke reduction [16]. However, this process is highly endothermic by nature and thus it requires more energy consumption [17]. CO_2 reforming has also been studied; for example, Zhang et al. [18] studied the H_2 production by CO_2 reforming of CH_4 using bimetallic CO–Zr/AC catalyst. The conversions of CO_2 and H_2 as well as syngas selectivity increased with increasing reaction temperature. Moreover, steam and CO_2 reforming of propane was investigated and proposed by Wang et al. [19]. It was found that CO_2 reforming had both benefit and drawback. The syngas ratio can be easily adjusted by controlling CO_2 through various feed ratios and complete conversion of propane can be reached. On the other hand, use of more CO_2 led to lower H_2 concentration in syngas product.

The combined processes of gasification and reforming have been studied by many researchers [20–22]. Gao et al. [20] investigated the updraft fixed bed gasifier combined with porous ceramic reformer for H_2-rich gas production from biomass. They found that H_2 yield was increased with increased gasification temperature and porous ceramic reformer helped reduce tar content. Wu et al. [21] studied the effect of various catalysts in combined steam gasification and reforming process using polypropylene for H_2 production. The Ni/MgO catalysts showed low activity for H_2 production; however, Ni/ZSM-5 zeolite offered high H_2 concentration in comparison with other catalysts. Additionally, polypropylene conversion and gas yield of catalytic reformer was higher than non-catalyzed process.

Our previous work studied the thermodynamic analysis of biomass gasification with CO_2 recycle, the results revealed that the CO_2 recycled process offered the potential benefits in terms of efficiency and energy [12]. In the present work, biochar is used as representative of biomass because of advantages such as high fixed carbon content and low volatility [23,24]. The thermodynamic analysis of different combined systems of gasifier, reformer and CO_2 capture unit for syngas production with steam, O_2 and CO_2 feed simultaneously is carried out by Aspen Plus software. The performance of each combined system under various operating temperature and feed ratios is analyzed and compared in terms of efficiency and CO_2 emissions. The efficiency is evaluated in terms of cold gas efficiency (CGE), gasification system efficiency (GSE), energy requirement and gaseous product composition. The combined systems investigated in this work consist of 1) conventional gasifier without CO_2 recycle (*Con-BG*), 2) conventional gasifier with CO_2 recycle (*Con-BG-reCO$_2$*), 3) combined gasifier and reformer without CO_2 recycle (*CBGR*), 4) combined gasifier and reformer with Post-CO_2 recycle (*CBGR-Post-reCO$_2$*) and 5) combined gasifier and reformer with Pre-CO_2 recycle (*CBGR-Pre-reCO$_2$*).

Process description

There are five combined systems considered in this work. Fig. 1a shows the conventional biochar gasifier without CO_2 recycle (*Con-BG*). It is a simple system that utilizes both O_2 and steam as gasifying agents. The second system, the conventional biochar gasifier with CO_2 recycle (*Con-BG-reCO$_2$*), is shown in Fig. 1b. This system is very similar to the first except that a portion of the cooled CO_2 is recycled to the gasifier, making three gasifying agents (O_2, steam, and CO_2) being simultaneously utilized in the gasification. The third system is the combined biochar gasifier and reformer without CO_2 recycle (*CBGR*) as shown in Fig. 1c. This system is similar to the first system but an additional reformer unit is installed before the CO_2 absorption unit to upgrade the syngas product. The fourth system is the combined biochar gasifier and reformer with Post-CO_2 recycle (*CBGR-Post-reCO$_2$*) as shown in Fig. 1d. It has the same configuration as the third system with partial recycle of the cooled CO_2 stream. The last system is combined gasifier and reformer with Pre-CO_2 recycle (*CBGR-Pre-reCO$_2$*) as shown in Fig. 1 e. This system is very similar to *CBGR-Post-reCO$_2$* system but the reformer is installed after the CO_2 absorption unit instead.

Mangrove tree charcoal was selected as the biochar feed in this work due to its availability in Thailand. Its characteristics was obtained by proximate and ultimate analysis. The steam used in the process is produced by passing water through a heat-exchanger. Oxygen, supplied from air purification process, is directly introduced to the gasifier. After the feedstock pretreatment, the biochar and mixture of gasifying agents were then fed to the gasifier. The gasifier effluent stream was passed to a CO_2 absorption unit. The CO_2 removal efficiency was assumed at 90% [25]. The absorbed CO_2 was cooled down

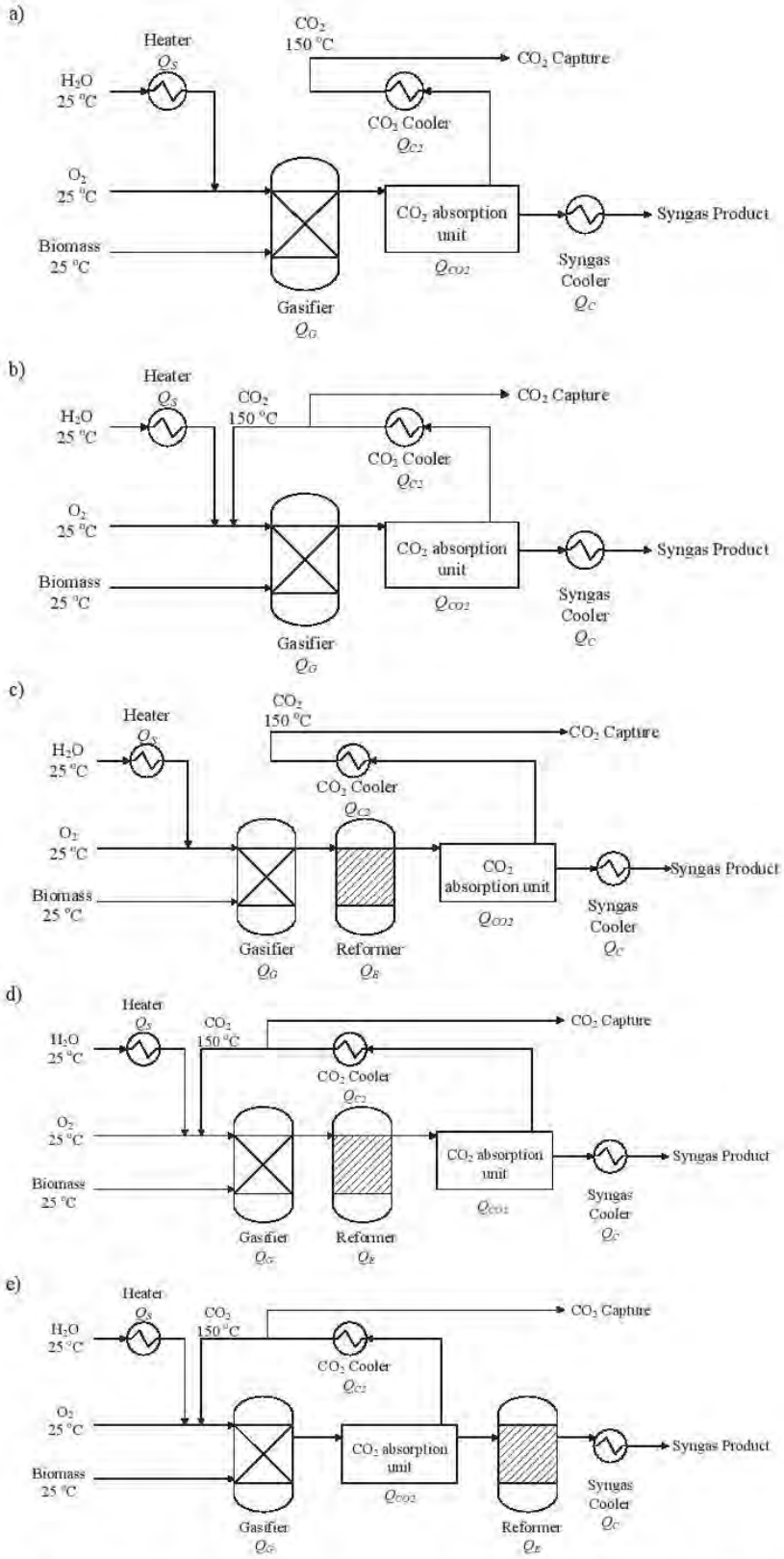

Fig. 1 – Process flow diagram a) conventional biomass gasifier without CO_2 recycle (*Con-BG*) b) conventional biomass gasifier with CO_2 recycle (*Con-BG-reCO₂*) c) combined biomass gasifier and reformer without CO_2 recycle (*CBGR*) d) combined biomass gasifier and reformer with Post-CO_2 recycle (*CBGR-Post-reCO₂*) e) combined biomass gasifier and reformer with Pre-CO_2 recycle (*CBGR-Pre-reCO₂*).

to 150 °C. Some of the cooled CO_2 was recycled (the amount was controlled by inlet CO_2/C ratio) to the gasifier and the remaining was calculated as the amount of CO_2 captured. A reformer unit may be required in some systems to upgrade the syngas product. The main reactions involved in the combined systems are illustrated as follows:

Reverse Boudouard reaction (*BD*):

$$C + CO_2 \leftrightarrow 2CO \quad \Delta H_r^0 = 172\ MJ/kmol \tag{1}$$

Partial oxidation (*PO*):

$$2C + O_2 \leftrightarrow 2CO \quad \Delta H_r^0 = -221\ MJ/kmol \tag{2}$$

Steam reforming (*SR*):

$$C + H_2O \leftrightarrow CO + H_2 \quad \Delta H_r^0 = 131\ MJ/kmol \tag{3}$$

Methane formation (*MF*):

$$C + 2H_2 \leftrightarrow CH_4 \quad \Delta H_r^0 = -74\ MJ/kmol \tag{4}$$

CO_2 reforming (*CR*):

$$CH_4 + CO_2 \leftrightarrow 2CO + 2H_2 \quad \Delta H_r^0 = 247\ MJ/kmol \tag{5}$$

Methane reforming (*MR*):

$$CH_4 + H_2O \rightarrow CO + 3H_2 \quad \Delta H_r^0 = 206\ MJ/kmol \tag{6}$$

Water gas shift (*WGS*):

$$CO + H_2O \leftrightarrow CO_2 + H_2 \quad \Delta H_r^0 = -41\ MJ/kmol \tag{7}$$

System modeling

Thermodynamic modeling of combined biomass gasification and reforming can be done by two methods. The first method is based on stoichiometric approach. This method has to specify a set of reactions occurring in the gasifier. The other method is based on non-stoichiometric approach, called Gibbs free energy minimization. This can be done by specifying only expected components of the product. Due to the complexity of gasification and reforming processes in real systems, it is very difficult to specify all the reactions that are involved. Therefore, this method is more preferable as it can be used to investigate the system behavior without the knowledge of reactions mechanism. Many studies have verified the modeling results with the experimental results and it was found that both methods showed the good agreement [26–28].

In this work, the non-stoichiometric approach was selected and carried out by using Aspen Plus software. The relevant components data were input into this model. The biochar was fed at 100 kg/h and its compositions were obtained from proximate and ultimate analysis. The steam and oxygen were simultaneously fed to gasifier. Gasification model was based on minimization of Gibbs free energy so the chemical equilibrium was reached. Gasification process consisted of decomposition and gasification section. Therefore, it can be simulated by using *RYield* reactor followed by *RGibbs* reactor. The *RYield* reactor was used to decompose biochar into elements (C, H, O). The yield of these elements was specified according to ultimate analysis of biochar. Then, the *RGibbs* reactor was used to simulate gasification section which was based on Gibb free energy minimization approach. The temperature of gasifier was set at 600 °C, adequate to achieve 100% carbon conversion of biochar. Noted that the solid ash product was separated and excluded from the model calculations. The other operating conditions are summarized in Table 1. CO_2 and steam reforming was operated at temperature between 600 and 1000 °C. *REquil* reactor was used to simulate reformer to convert remaining hydrocarbon from gasifier to syngas product. The CO_2 absorption unit was represented by ideal separation block, set at 90% CO_2 recovery. The absorbed CO_2 stream obtained from the CO_2 absorption unit was then sent to a splitter unit where a portion or all of it was sent back to the gasifier for controlling the feed ratio and the remaining CO_2 was indicated as CO_2 capture.

In this study, the major operating parameters are the reformer temperature and utilizer feed ratio. The performance of the five types of combined systems is evaluated and compared in terms of efficiency, energy requirement and CO_2 emission. The evaluation parameters are H_2 mole fraction, cold gas efficiency (*CGE*) (Eq. (8)), H_2/CO ratio, CO_2 emission ratio (CO_2 *EMR*) (Eq. (12)), total net heat requirement (Eq. (13)) and gasification system efficiency (*GSE*) (Eq. (14)). The cold gas efficiency (*CGE*) (Eq. (8)) is generally used for evaluating the quality of syngas from different biochar sources and is defined as [13].

$$CGE\ (-) = \frac{M_{syngas} LHV_{syngas}}{M_{biochar} LHV_{biochar}} \tag{8}$$

where

$$LHV_{biomass}(MJ/kg) = \frac{M_{biomass} HHV_{biomass} - 0.5 M_H L_{298}}{M_{biomass}} \tag{9}$$

$$LHV_{syngas}(MJ/kg) = \frac{n_{CO} H^0_{CO,298} + n_{H_2} H^0_{H_2,298} + n_{CH_4} H^0_{CH_4,298}}{M_{syngas}} \tag{10}$$

For the high heating value of biochar ($HHV_{biochar}$), it can be calculated by using the correlation proposed by Channiwala and Parikh [29] as illustrated in Eq. (11).

$$HHV\ (MJ/kg) = 0.3491x_C + 1.1783x_H - 0.1034x_O \tag{11}$$

In case of environmental evaluation, we propose the CO_2 emission ratio (CO_2 *EMR*) as an indicator. This is the fraction of

Table 1 – Operating conditions and input data.

Feedstock	Charcoal ($CH_{0.78}O_{0.33}$)
Inlet temperature of biomass and O_2	25 °C
Inlet temperature of CO_2	150 °C
Inlet temperature of steam	327 °C
Gasifier temperature	600 °C
Pressure	1 atm
O_2/C	0–0.5
S/C	0–2
CO_2/C	0–1
Stream class	MCINCPSD[a]
Valid- phases	Vapor-Liquid[a]
Thermodynamics properties	Peng-Robinson[a]
NC Props	
Enthalpy	HCOALGEN (code 6)[a]
Density	DCOALIGT[a]

[a] Aspen Plus software parameters.

CO_2 emission released to environment divided by total CO_2 produced by process. When this ratio is equal to 1, it means that all CO_2 emission is released from the process. On the other hand, when this value is equal to 0, it means that no CO_2 emission is released from the process.

$$CO_2\ emission\ ratio\ (CO_2\ EMR) = \frac{CO_2\ emission}{CO_2\ total} \quad (12)$$

In term of energy requirement, it is represented by total net heat of process which is summation of heat duty of each unit adding with syngas enthalpy. The positive value shows that the energy is required for the process. The negative value shows that the energy is produced by the process.

$$Total\ net\ heat = Q_{syngas} + Q_G + Q_E + Q_S + Q_{CO_2} + Q_C + Q_{C2} \quad (13)$$

where Q_{syngas} is heat of combustion of syngas (MJ/h), Q_G is energy required for gasifier (MJ/h), Q_E is energy required for reformer (MJ/h), Q_S is energy required for steam generator (MJ/h), Q_{CO2} is energy required for CO_2 absorption unit (MJ/h), Q_C is energy required for syngas cooler (MJ/h) and Q_{C2} is energy required for CO_2 cooler (MJ/h).

In previous work, we proposed the gasification system efficiency (GSE) to take energy requirement into account [12].

$$GSE = \frac{Energy\ output\ of\ each\ unit}{Energy\ input\ of\ each\ unit} \quad (14)$$

The energy required for CO_2 absorption unit (Q_{CO2}) is calculated by using the data proposed by Peters et al. [25] which is equal to 3 MJ/kg of CO_2 captured by amine absorption process.

The model validation is carried out and compared to other literature. As shown in Table 2, for biochar of $CH_{1.4}O_{0.6}$, $CO_2/C = 0.5$ and $P = 1$ atm, the results are in good agreement with the results of Chaiwatanodom et al. [12], Renganathan et al. [13]. In addition, the validation with Gao et al. [20] shows that the simulations could predict the experimental results particularly at high temperature.

Table 2 – Model validation. (Biomass $CH_{1.4}O_{0.6}$, $CO_2/C = 0.5$ and $P = 1$ atm).

	[12]	[13]	This work	%Error [12]	%Error [13]
T = 800 °C					
y_{H2}	0.310	0.307	0.311	0.32	1.23
y_{CO}	0.598	0.600	0.598	0.00	0.39
y_{CO2}	0.090	0.098	0.089	1.01	8.99
y_{CH4}	0.043	0.000	0.002	94.54	n/a
T = 1000 °C					
y_{H2}	0.303	0.290	0.304	0.33	4.68
y_{CO}	0.624	0.625	0.624	0.05	0.19
y_{CO2}	0.073	0.081	0.073	0.97	10.38
y_{CH4}	0.059	0.000	0.000	n/a	n/a
T = 1200 °C					
y_{H2}	0.294	0.290	0.296	0.46	1.95
y_{CO}	0.643	0.650	0.642	0.08	1.18
y_{CO2}	0.063	0.067	0.062	1.31	7.49
y_{CH4}	0.071	0.000	0.000	n/a	n/a

	[20]	This work	%Error [20]
T = 850 °C			
y_{H2}	0.450	0.605	34.44
y_{CO}	0.220	0.206	6.45
y_{CO2}	0.240	0.189	21.18
y_{CH4}	0.080	0.000	n/a
T = 900 °C			
y_{H2}	0.470	0.600	27.77
y_{CO}	0.220	0.220	0.00
y_{CO2}	0.220	0.180	18.24
y_{CH4}	0.070	0.000	n/a
T = 950 °C			
y_{H2}	0.560	0.596	6.49
y_{CO}	0.210	0.232	10.60
y_{CO2}	0.180	0.171	4.80
y_{CH4}	0.060	0.000	n/a

Table 3 – Proximate and ultimate analysis of mangrove tree charcoal.

Proximate (wt%)	
Moisture	5.30
Volatile matters	36.26
Fixed carbon	56.40
Ash	2.05
Ultimate (wt%)	
C	66.46
H	4.37
O (balance)	29.14
N	0.03
High heating value (MJ/kg)[a]	25.337

[a] Using correlation proposed by Channiwala and Parikh [29].

Results and discussions

Biochar characterization

The biochar was characterized using proximate and ultimate analysis to obtain the initial data of feedstock for simulations. Table 3 shows the characterization results of the biochar.

The simulation results were analyzed and the performance of different combined systems was compared as follows.

Comparison of Con-BG *and* Con-BG-reCO$_2$

The results of H_2 fraction & CGE, and H_2/CO ratio & CO_2 EMR for the conventional systems (no reformer unit) are illustrated in Fig. 2a and Fig. 2b, respectively, as the black and white marks. It should be noted that there is no variation in reformer temperature in both systems because they do not have a reformer unit and complete carbon conversion can be achieved at temperature of 600 °C. It can be seen from Fig. 2a that the H_2 fraction of the *Con-BG* system (black triangle mark) is higher than the fraction of the *Con-BG-reCO$_2$* system (black circle mark). This is because the recycled stream of CO_2 contributes to a high CO content in the syngas product via Boudouard (BD) and reverse water gas shift reaction (rWGS). However, the *Con-BG-reCO$_2$* system (white circle mark) offers a higher CGE compared to the *Con-BG* system (white triangle mark). The reason is because large amount of CO is obtained in the syngas product of the *Con-BG* system. In case of H_2/CO ratio, as shown in Fig. 2b, the *Con-BG-reCO$_2$* system is found to produce more CO content in the syngas product. Therefore, its

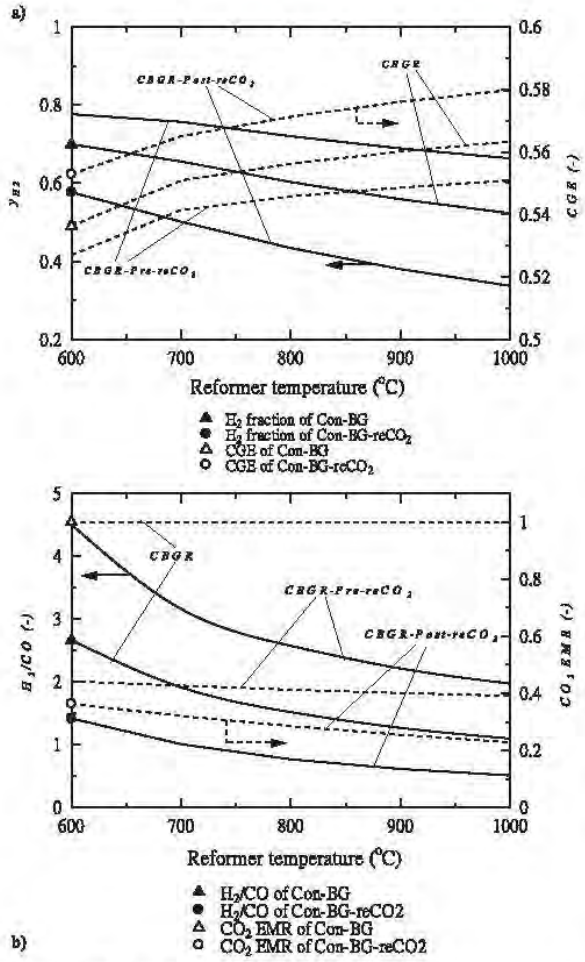

Fig. 2 – Effects of reformer temperature on various type of operating mode ($O_2/S/CO_2/C = 0.5/1/1/1$) a) H_2 fraction with CGE b) H_2/CO ratio with CO_2 EMR.

H_2/CO ratio is lower than that of the Con-BG system. Nevertheless, the Con-BG-$reCO_2$ offers more benefit in term of CO_2 EMR because some CO_2 can be captured and recycled in the process and thus the CO_2 emission is lower.

Comparison of Con-BG *and* CBGR

The CBGR system consists of gasifier and reformer; therefore, reformer temperature can be varied. The Con-BG (black triangle mark) provides higher H_2 fraction when compared with the CBGR at all ranges of reformer temperature as illustrated in Fig. 2a. This is because more CO content is produced in gaseous product by the reformer. Moreover, increasing reformer temperature also reduces the H_2 fraction due to the endothermic behavior of reverse water gas shift reaction (rWGS). On the other hand, the presence of reformer unit provides higher CGE for the CBGR system as compared to the CGE obtained from the Con-BG system (white triangle mark). In addition, the CGE of the CBGR system can be increased with an increase in reformer temperature. In conclusion, the combination of gasifier and reformer can improve the performance in term of CGE of gaseous product. In Fig. 2b, H_2/CO ratio of the Con-BG (black triangle mark) is higher than that of the CBGR system. This is simply because the reformer unit produces more CO content. Moreover, it can be seen that H_2/CO ratio is decreased with an increase in the reformer temperature. In term of CO_2 EMR, the results for both systems are the same because there is no recycle stream of CO_2 as all the captured CO_2 is released.

Comparison of CBGR *and* CBGR-Post-$reCO_2$

For the effect of reformer temperature, it is clearly seen that the H_2 fraction of the CBGR system is higher than that of the CBGR-Post-$reCO_2$ system as shown in Fig. 2a. This is because the CBGR-Post-$reCO_2$ system produces more CO via recycled CO_2 from the process. However, high amount of CO leads to a high CGE of the gaseous product as can be observed in Fig. 2a. Although increasing the reformer temperature reduces H_2 content, it can increase the CGE. From Fig. 2b, the H_2/CO ratio of the CBGR is higher than the CBGR-Post-$reCO_2$ system because of the same reason as described in the H_2 fraction parameter. A clear advantage of the CBGR-Post-$reCO_2$ system over the CBGR system is that it can reduce the CO_2 emission as shown in Fig. 2b. The CO_2 EMR of the CBGR-Post-$reCO_2$ system is much lower than that of the CBGR system due to the utilization of captured CO_2 as a gasifying agent. In addition, it was found that the CO_2 EMR can be lower if the reformer temperature is increased. This is a result of the endothermic reaction behavior of Boudouard reaction (BD), CO_2 reforming reaction (CR) and reverse water gas shift reaction (rWGS), thus more CO_2 is consumed. In overall, the CBGR-Post-$reCO_2$ system shows better performance in terms of both efficiency and environment. In the next section, the effect of O_2/C ratio on the performance of both systems will be investigated. Due to the slight increase in CGE and sharp decrease in H_2 fraction with reformer temperature over 700 °C, the reformer temperature of 700 °C is fixed as the base case temperature.

The influence of O_2/C ratio is illustrated in Fig. 3. In general, the CBGR system offers a higher H_2 fraction but lower CGE as compared to those of the CBGR-Post-$reCO_2$ system, at all O_2/C ratios. Increasing the O_2/C ratio decreases the H_2 fraction and produces higher CO content. However, it is an opposite trend when the O_2/C ratio is higher than 0.2. This may be because the partial oxidation (PO) reaction has a significant impact on the process at low O_2/C ratio. For the effect on CGE, it was also found that the O_2/C ratio of 0.2 is a turning point for the CBGR-Post-$reCO_2$ system, giving the highest CGE. However, over the O_2/C ratio of 0.2, the CGE decreases sharply. In case of the CBGR system, it can be noticed that the CGE is rather stable at low O_2/C ratio. However, the CGE decreases sharply when O_2/C ratio is roughly higher than 0.25. This is because, beyond this ratio, more CO_2 is produced via combustion reaction rather than gasification.

From Fig. 3b, the H_2/CO ratio for both CBGR and CBGR-Post-$reCO_2$ systems shows a similar trend, with a lower H_2/CO ratio for the CBGR-Post-$reCO_2$ system. It can be seen that at low O_2/C ratios, the H_2/CO ratio tends to decrease with an increase in O_2/C ratio. This result offers benefit in term of using syngas with low H_2/CO ratio for suitable application. It can be

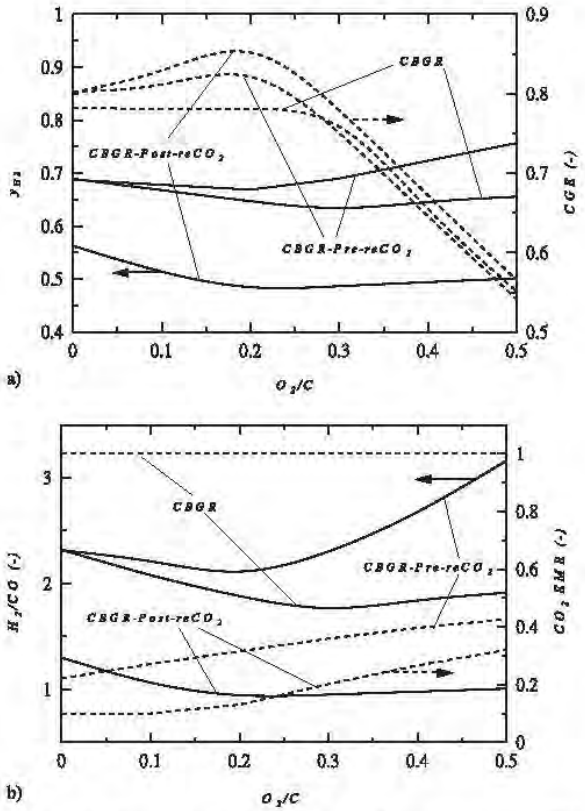

Fig. 3 – Effects of O_2/C on various type of operating mode ($S/CO_2/C = 1/1/1$ and Reformer temperature = 700 °C) a) H_2 fraction with CGE b) H_2/CO ratio with CO_2 EMR.

observed that the CBGR-Post-reCO_2 system produces more CO_2 when the O_2/C ratio was greater than 0.2. This is supported by the curve CO_2 EMR which shows a sharp slope as illustrated in Fig. 3b. Therefore, the O_2/C ratio of 0.2 is the pivot point for converting between CO and CO_2.

Comparison of CBGR-Post-reCO_2 *and* CBGR-Pre-reCO_2

The results from the previous sections shows that the presence of CO_2 recycle stream offers the benefit in terms of both efficiency and environment. In this section, it is interesting to investigate and compare performance of the combined systems with different locations of CO_2 absorption unit; that is, before and after the reformer unit. It is expected that installing the CO_2 absorption unit before the reformer can improve the reformer performances and also reduce energy requirement of the system. For the effect of reformer temperature as shown in Fig. 2a, compared to the CBGR-Post-reCO_2 system, the CBGR-Pre-reCO_2 system offers a higher H_2 fraction but lower CGE. Also, when the reformer temperature is increased, the H_2 fraction is decreased while the CGE is increased for both systems. The reason is because more CO is produced at higher reformer temperature. In addition, it was found that the CBGR-Pre-reCO_2 system produces higher amount of H_2 than the CBGR-Post-reCO_2 system. This is because in the CBGR-Pre-reCO_2 system CO_2 is removed from the gasifier effluent prior to feeding to the reformer unit. Since steam reforming (SR) is a main reaction in the CBGR-Pre-reCO_2 system. Because of CO_2 removal, it leads to production of more H_2 in the gaseous product by steam reforming and WGSR. From Fig. 2b, it is found that the H_2/CO ratio of the CBGR-Pre-reCO_2 system is higher than that of the CBGR-Post-reCO_2 system due to the same reason as explained above. In addition, the CBGR-Post-reCO_2 system offers more potential in term of environment as seen in the CO_2 EMR parameter. This is because the CO_2 absorption unit can absorb 90% CO_2 before discharging from the process. Compared with the CBGR-Pre-reCO_2 system, the CO_2 produced from the reformer unit is not absorbed.

The effect of O_2/C ratio on H_2 fraction and CGE is shown in Fig. 3a. The CBGR-Pre-reCO_2 provides the highest H_2 fraction because CO_2 is removed before being fed to the reformer. Furthermore, this system can increase the H_2 content due to the effect of steam reforming reaction. The CBGR-Post-reCO_2 system offers the lowest of H_2 fraction because the presence of CO_2 in the reformer is an inhibiter for the WGSR, leading to more CO produced. H_2 fraction is decreased with an increase in O_2/C ratio at the range of 0–0.2. However, the H_2 fraction is increased when the O_2/C ratio is above 0.2. This trend can be observed in both CBGR-Pre-reCO_2 and CBGR-Post-reCO_2 systems. It can be explained that O_2 is used in partial oxidation (PO) to produce CO. This phenomenon causes the reduction of H_2 fraction for the O_2/C ratio below 0.2. On the other hand, at the O_2/C ratio above 0.2 the combustion reaction generating CO_2 instead of CO gains dominant role. In term of CGE, the CBGR-Post-reCO_2 provides higher CGE than that of the CBGR-Pre-reCO_2 system due to the presence of more CO content in gaseous product. In addition, it can be observed that the highest CGE is obtained at O_2/C ratio of 0.2 for both systems. The effect of O_2/C ratio to the H_2/CO ratio is shown in Fig. 3b. It is shown that the CBGR-Pre-reCO_2 system offers the highest H_2/CO ratio while the CBGR-Post-reCO_2 system provides the lowest of H_2/CO ratio. Nevertheless, in the view of environmental concern, the CBGR-Post-reCO_2 system offers a lower CO_2 EMR than the CBGR-Pre-reCO_2 system. In addition, increasing O_2/C ratio produces more CO_2 EMR due to the additional CO_2 produced via combustion.

Fig. 4 illustrates the effects of S/C and CO_2/C ratios on the H_2 content and CGE of the CBGR-Post-reCO_2 system. It is found that CO_2/C ratio reaches the maximum value of 0.6 at the S/C ratio of 0 due to the insufficient amount of recycled CO_2 as showed in Fig. 4a. It can be noticed that the CBGR-Post-reCO_2 system generally provides the H_2 content less than that of CBGR-Pre-reCO_2 system due to the presence of more CO_2 in reformer unit. However, it can offer a slightly higher CGE. The effect of S/C ratio is in similar trend as the CBGR-Pre-reCO_2 system. The CGE was found to achieve the maximum value at the S/C ratio of 1.2. The performance of CO_2 EMR and H_2/CO were studied and shown in Fig. 4b. It can be noticed that the CO_2 EMR value less than 0.2 can be achieved by the CBGR-Post-reCO_2 system. The H_2/CO ratio below 1 can be obtained at low S/C and high CO_2/C. To determine the energy requirement of a system, total net heat is calculated from all the main units comprised in the system, as described in equation (13). The calculation results of the CBGR-Pre-reCO_2 and CBGR-Post-reCO_2 systems are illustrated in Tables 4–7. It should be noted that

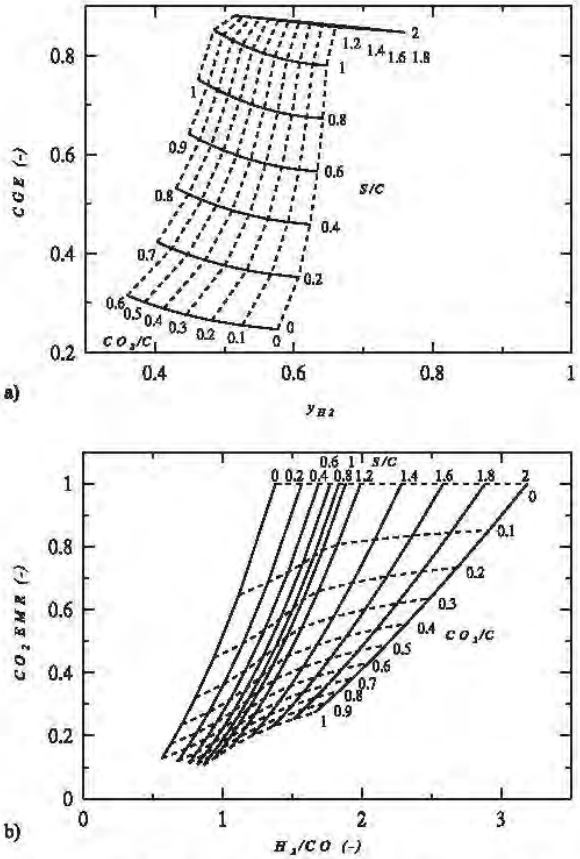

Fig. 4 – Effects of S/C and CO_2/C on CBGR-Post-reCO_2 (O_2/C = 0.2/1 and Reformer temperature = 700 °C) a) H_2 fraction with CGE b) H_2/CO ratio with CO_2 EMR.

the positive values indicate energy requirement while the negative values indicate energy production by the system. In general, for both systems, it is found that the total net heat of CBGR-Post-reCO_2 reaches maximum value at the S/C ratio of 1.2 and tends to decrease when the S/C ratio is higher due to the energy requirement of steam generation unit. Moreover, it is also found that the CBGR-Post-reCO_2 system typically offers higher total net heat than that of CBGR-Pre-reCO_2 system because more CO is produced via CBGR-Post-reCO_2. Increasing CO_2/C ratio is found to decrease the total net heat because of more energy requirement at CO_2 absorption unit. For Table 5, likewise the CBGR-Pre-reCO_2 system, GSE is found to be increased to maximum value at S/C of 1.2 and decreases subsequently afterward.

The effects of S/C and CO_2/C ratios on the H_2 fraction and CGE of CBGR-Pre-reCO_2 are shown in Fig. 5a. It can be seen that increasing CO_2/C ratio can increase the CGE but decrease the H_2 fraction as a result of more CO produced. However, increasing the S/C ratio can increase both of CGE and H_2 fraction. This is because the addition of more steam in the gasifier shifts the equilibrium of steam reforming (SR) and water gas shift (WGS) reactions and thus produces more H_2. However, this effect becomes insignificant when the S/C feed ratio exceeds 1.2 as the CGE reaches the maximum limit of 0.83. Fig. 5b shows the effect of S/C and CO_2/C ratios on CO_2 EMR and H_2/CO. It is found that the CO_2 EMR is decreased as the CO_2/C feed ratio increases due to the presence of more CO_2 recycled in the process. On the other hand, increasing the S/C feed ratio results in more CO_2 EMR due to the additional CO_2 produced from water gas shift reaction. It can be noticed that, in case of no steam supplied (S/C ratio is 0), the H_2/CO ratio can be adjusted to be lower than 2.8 by increasing the CO_2/C ratio. Table 6 shows total net heat of CBGR-Pre-reCO_2 at various CO_2/C and S/C feed ratio. It can be seen that increasing S/C offers more energy production. However, when the ratio was over 1.2 it shows the reversal effect. Increasing CO_2/C causes the total net heat to be decreased. This is because more energy is required at the CO_2 absorption unit as more CO_2 is produced from the gasifier effluent. Table 7 shows the GSE of CBGR-Pre-reCO_2 system at various S/C molar ratio and CO_2/C molar ratios. Similar to the total net heat result, it is found that the GSE reaches the peak value at the S/C ratio of around 1.2. In the view of CO_2/C ratio, the GSE is not significantly decreased when increasing the CO_2/C feed ratio.

It can be summarized that the CBGR-Pre-reCO_2 system offers more H_2 fraction than the CBGR-Post-reCO_2 system because there is less amount of CO_2 in the reformer (less effect of reversed water gas shift reaction). However, the CGE obtained by the CBGR-Post-reCO_2 system is slightly higher due to the presence of CO. For H_2/CO ratio, the CBGR-Post-reCO_2 system can produce syngas with the ratio less than 1, but the H_2/CO ratio of the CBGR-Pre-reCO_2 system can be as high as 8.

Table 4 – Total net heat (MJ/hr) of CBGR-Post-reCO_2 at various S/C molar ratio and CO_2/C molar ratio.

CO_2/C	S/C										
	0	0.2	0.4	0.6	0.8	1	1.2	1.4	1.6	1.8	2
0	−1145	−1293	−1440	−1588	−1735	−1883	−1982	−1956	−1930	−1906	−1885
0.1	−1118	−1266	−1413	−1561	−1708	−1856	−1957	−1926	−1898	−1873	−1849
0.2	−1092	−1239	−1386	−1534	−1681	−1829	−1928	−1895	−1865	−1837	−1812
0.3	−1066	−1212	−1359	−1507	−1654	−1802	−1898	−1862	−1829	−1800	−1774
0.4	−1041	−1186	−1333	−1480	−1627	−1775	−1864	−1827	−1793	−1763	−1735
0.5	−1016	−1161	−1306	−1453	−1600	−1748	−1829	−1790	−1755	−1723	−1695
0.6	−992	−1135	−1280	−1427	−1574	−1721	−1792	−1752	−1716	−1683	−1654
0.7	n/a	−1110	−1255	−1401	−1547	−1694	−1754	−1712	−1675	−1642	−1613
0.8	n/a	n/a	−1229	−1375	−1521	−1667	−1714	−1671	−1634	−1600	−1570
0.9	n/a	n/a	n/a	−1349	−1495	−1641	−1672	−1630	−1591	−1557	−1527
1	n/a	n/a	n/a	n/a	−1469	−1615	−1630	−1587	−1548	−1514	−1483

Table 5 – GSE of (–) CBGR-Post-reCO$_2$ at various S/C molar ratio and CO$_2$/C molar ratio.

CO$_2$/C	S/C										
	0	0.2	0.4	0.6	0.8	1	1.2	1.4	1.6	1.8	2
0	0.495	0.569	0.638	0.703	0.763	0.820	0.856	0.846	0.838	0.832	0.827
0.1	0.492	0.564	0.632	0.696	0.755	0.811	0.847	0.837	0.830	0.824	0.819
0.2	0.491	0.561	0.627	0.689	0.748	0.803	0.839	0.829	0.822	0.816	0.811
0.3	0.490	0.558	0.623	0.684	0.741	0.795	0.830	0.821	0.813	0.808	0.803
0.4	0.490	0.556	0.619	0.679	0.735	0.789	0.821	0.812	0.805	0.800	0.795
0.5	0.490	0.554	0.616	0.674	0.730	0.783	0.812	0.803	0.797	0.791	0.787
0.6	0.491	0.553	0.613	0.670	0.725	0.777	0.803	0.795	0.788	0.783	0.779
0.7	n/a	0.552	0.611	0.667	0.720	0.771	0.794	0.786	0.780	0.775	0.771
0.8	n/a	n/a	0.609	0.664	0.716	0.766	0.785	0.777	0.771	0.767	0.763
0.9	n/a	n/a	n/a	0.661	0.712	0.762	0.776	0.769	0.763	0.759	0.755
1	n/a	n/a	n/a	n/a	0.709	0.757	0.767	0.760	0.755	0.751	0.747

Table 6 – Total net heat (MJ/hr) of CBGR-Pre-reCO2 at various S/C molar ratio and CO$_2$/C molar ratio.

CO$_2$/C	S/C										
	0	0.2	0.4	0.6	0.8	1	1.2	1.4	1.6	1.8	2
0	−1081	−1207	−1332	−1458	−1583	−1709	−1805	−1809	−1803	−1792	−1778
0.1	−1048	−1172	−1296	−1422	−1547	−1673	−1768	−1768	−1760	−1747	−1733
0.2	−1017	−1138	−1262	−1386	−1511	−1637	−1730	−1727	−1716	−1702	−1687
0.3	−987	−1106	−1229	−1352	−1477	−1601	−1691	−1684	−1672	−1656	−1640
0.4	−958	−1076	−1196	−1319	−1443	−1567	−1651	−1641	−1627	−1610	−1593
0.5	−929	−1046	−1165	−1287	−1409	−1533	−1611	−1598	−1582	−1564	−1546
0.6	−902	−1016	−1135	−1255	−1377	−1500	−1569	−1554	−1536	−1517	−1498
0.7	−875	−988	−1105	−1224	−1345	−1467	−1527	−1509	−1490	−1470	−1450
0.8	−849	−960	−1075	−1193	−1314	−1435	−1484	−1464	−1443	−1422	−1401
0.9	n/a	−932	−1047	−1164	−1283	−1403	−1440	−1418	−1396	−1374	−1353
1	n/a	−905	−1018	−1134	−1252	−1372	−1396	−1372	−1349	−1326	−1304

Table 7 – GSE (–) of CBGR-Pre-reCO$_2$ at various S/C molar ratio and CO$_2$/C molar ratio.

CO$_2$/C	S/C										
	0	0.2	0.4	0.6	0.8	1	1.2	1.4	1.6	1.8	2
0	0.480	0.551	0.617	0.678	0.736	0.790	0.824	0.815	0.808	0.803	0.799
0.1	0.476	0.544	0.608	0.668	0.725	0.778	0.813	0.804	0.798	0.793	0.789
0.2	0.473	0.538	0.601	0.660	0.716	0.768	0.803	0.794	0.788	0.783	0.780
0.3	0.471	0.534	0.595	0.653	0.708	0.759	0.792	0.784	0.778	0.773	0.770
0.4	0.470	0.531	0.590	0.647	0.700	0.751	0.782	0.774	0.768	0.763	0.760
0.5	0.469	0.528	0.586	0.641	0.694	0.744	0.772	0.764	0.758	0.754	0.751
0.6	0.469	0.526	0.582	0.636	0.687	0.737	0.761	0.754	0.748	0.744	0.742
0.7	0.469	0.524	0.579	0.632	0.682	0.730	0.751	0.744	0.739	0.735	0.733
0.8	0.469	0.523	0.576	0.627	0.677	0.724	0.742	0.735	0.730	0.726	0.724
0.9	n/a	0.522	0.574	0.624	0.672	0.719	0.732	0.725	0.721	0.717	0.715
1	n/a	0.521	0.571	0.621	0.668	0.714	0.723	0.716	0.712	0.708	0.706

Thus, it can be said that the CBGR-Pre-reCO$_2$ system offers a wide range of H$_2$/CO ratio for syngas applications. In term of environment performance, increasing the CO$_2$/C ratio can generally reduce the CO$_2$ emission and the CO$_2$ EMR can reach the minimum value of 0.1 via the CBGR-Post-reCO$_2$ system. In term of energy requirement, the CBGR-Post-reCO$_2$ system can produce more energy than the CBGR-Pre-reCO$_2$ system because more CO is produced by CBGR-Post-reCO$_2$, resulting in more syngas energy (via heat of combustion). In the similar trend, the GSE of the CBGR-Post-reCO$_2$ system is slightly higher than the GSE of the CBGR-Pre-reCO$_2$ system due to the same reason as the energy requirement.

Conclusions

The Con-BG, Con-BG-reCO$_2$, CBGR, CBGR-Post-reCO$_2$ and CBGR-Pre-reCO$_2$ systems have been investigated at various reformer temperatures and feed ratios. The results reveal that the conventional gasifier types have the limitation in varying the temperature. However, for the combined systems of gasifier and reformer (including CBGR, CBGR-Post-reCO$_2$ and CBGR-Pre-reCO$_2$) can increase the CGE and decrease the CO$_2$ EMR by increasing the reformer temperature. The CBGR system is inferior in term of CO$_2$ emission. For the effect of O$_2$/C feed

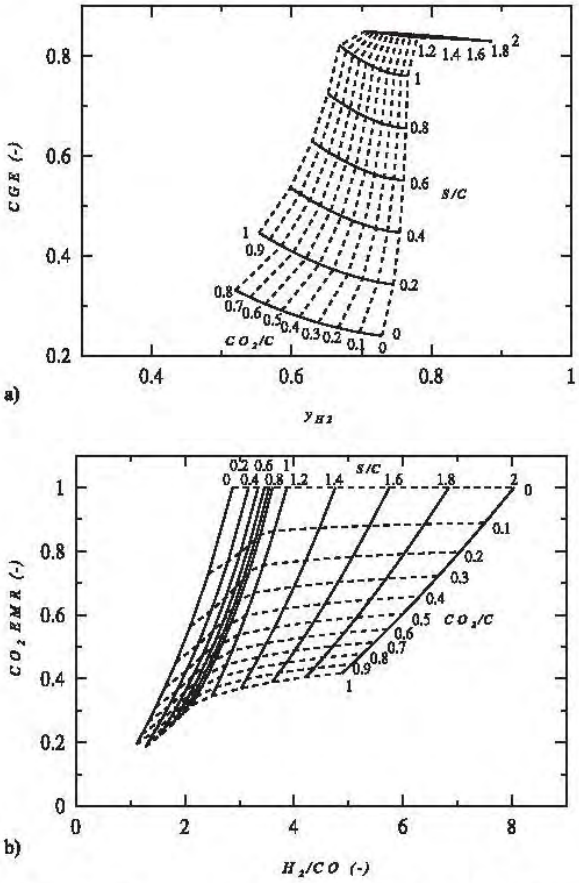

Fig. 5 – Effects of S/C and CO_2/C on CBGR-*Pre-reCO*$_2$ (O_2/C = 0.2/1 and Reformer temperature = 700 °C) a) H_2 fraction with CGE b) H_2/CO ratio with CO_2 EMR.

ratio, the best ratio is found at 0.2. Increasing the ratio over 0.2 causes the *CGE* to be decreased. The highest *CGE* can be obtained from the CBGR-*Post-reCO*$_2$ system but its H_2 fraction is lowest compared to other systems. To obtain the highest H_2 fraction, the CBGR-*Pre-reCO*$_2$ system is recommended. Increasing the O_2/C ratio results in increased CO_2 *EMR* due to the increased CO_2 through combustion reaction. For effect of S/C and CO_2/C ratios, it is found that *CGE* can achieve the maximum value at the S/C ratio of 1.2. Increasing CO_2/C not only reduces the CO_2 *EMR* but also produces the syngas with lower H_2/CO ratio. In term of energy requirement, the CBGR-*Post-reCO*$_2$ system provides more total net heat and *GSE* compared to the CBGR-*Pre-reCO*$_2$ system. Finally, CBGR-*Pre-reCO*$_2$ is a suitable system to produce the syngas with high H_2 fraction, while the CBGR-*Post-reCO*$_2$ system is appropriate for low H_2/CO ratio syngas.

Acknowledgment

The support from The Thailand Research Fund (TRG5780233) is gratefully acknowledged.

REFERENCES

[1] Khine MSS, Chen L, Zhang S, Lin J, Jiang SP. Syngas production by catalytic partial oxidation of methane over (La0.7A0.3)BO3 (A=Ba, Ca, Mg, Sr, and B=Cr or Fe) perovskite oxides for portable fuel cell applications. Int J Hydrogen Energy 2013;38:13300–8.
[2] Hackett GA, Gerdes K, Song X, Chen Y, Shutthanandan V, Engelhard M, et al. Performance of solid oxide fuel cells operated with coal syngas provided directly from a gasification process. J Power Sources 2012;214:142–52.
[3] Mondal P, Dang GS, Garg MO. Syngas production through gasification and cleanup for downstream applications — Recent developments. Fuel Process Technol 2011;92:1395–410.
[4] Heidi CB, Marco JC. CO_2 as a carbon neutral fuel source via enhanced biomass gasification. Environ Sci Technol 2009;43:9030–7.
[5] Cao Y, Wang Y, Riley JT, Pan W-P. A novel biomass air gasification process for producing tar-free higher heating value fuel gas. Fuel Process Technol 2006;87:343–53.
[6] Zhang B, Zhang L, Yang Z, Yan Y, Pu G, Guo M. Hydrogen-rich gas production from wet biomass steam gasification with CaO/MgO. Int J Hydrogen Energy 2015;40:8816–23.
[7] Reddy SN, Nanda S, Dalai AK, Kozinski JA. Supercritical water gasification of biomass for hydrogen production. Int J Hydrogen Energy 2014;39:6912–26.
[8] Cheng G, He P-w, Xiao B, Hu Z-q, Liu S-m, Zhang L-g, et al. Gasification of biomass micron fuel with oxygen-enriched air: thermogravimetric analysis and gasification in a cyclone furnace. Energy 2012;43:329–33.
[9] Schuster G, Loffler G, Weigl K, Hofbauer H. Biomass steam gasification - an extensive parametric modeling study. Bioresour Technol 2001;77:71–9.
[10] Moghtaderi B. Effects of controlling parameters on production of hydrogen by catalytic steam gasification of biomass at low temperatures. Fuel 2007;86:2422–30.
[11] Wei L, Xu S, Zhang L, Liu C, Zhu H, Liu S. Steam gasification of biomass for hydrogen-rich gas in a free-fall reactor. Int J Hydrogen Energy 2007;32:24–31.
[12] Chaiwatanodom P, Vivanpatarakij S, Assabumrungrat S. Thermodynamic analysis of biomass gasification with CO_2 recycle for synthesis gas production. Appl Energy 2014;114:10–7.
[13] Renganathan T, Yadav MV, Pushpavanam S, Voolapalli RK, Cho YS. CO_2 utilization for gasification of carbonaceous feedstocks: a thermodynamic analysis. Chem Eng Sci 2012;83:159–70.
[14] Roberts DG, Harris DJ. Char gasification in mixtures of CO_2 and H_2O: competition and inhibition. Fuel 2007;86:2672–8.
[15] Di Carlo A, Borello D, Sisinni M, Savuto E, Venturini P, Bocci E, et al. Reforming of tar contained in a raw fuel gas from biomass gasification using nickel-mayenite catalyst. Int J Hydrogen Energy 2015;40:9088–95.
[16] Antzara A, Heracleous E, Bukur DB, Lemonidou AA. Thermodynamic analysis of hydrogen production via chemical looping steam methane reforming coupled with in situ CO_2 capture. Int J Greenh Gas Control 2015;32:115–28.
[17] Tomishige K, Asadullah M, Kunimori K. Syngas production by biomass gasification using Rh/CeO2/SiO_2 catalysts and fluidized bed reactor. Catal Today 2004;89:389–403.
[18] Zhang G, Hao L, Jia Y, du Y, Zhang Y. CO_2 reforming of CH_4 over efficient bimetallic Co–Zr/AC catalyst for H_2 production. Int J Hydrogen Energy 2015;40:12868–79.
[19] Wang X, Wang N, Zhao J, Wang L. Thermodynamic analysis of propane dry and steam reforming for synthesis gas or hydrogen production. Int J Hydrogen Energy 2010;35:12800–7.

[20] Gao N, Li A, Quan C, Gao F. Hydrogen-rich gas production from biomass steam gasification in an updraft fixed-bed gasifier combined with a porous ceramic reformer. Int J Hydrogen Energy 2008;33:5430–8.
[21] Wu C, Williams PT. Hydrogen production by steam gasification of polypropylene with various nickel catalysts. Appl Catal B Environ 2009;87:152–61.
[22] Wu C, Wang Z, Huang J, Williams PT. Pyrolysis/gasification of cellulose, hemicellulose and lignin for hydrogen production in the presence of various nickel-based catalysts. Fuel 2013;106:697–706.
[23] Puig-Arnavat M, Bruno JC, Coronas A. Review and analysis of biomass gasification models. Renew Sustain Energy Rev 2010;14:2841–51.
[24] Gujar AC, Baik J, Garceau N, Muradov N, T-Raissi A. Oxygen-blown gasification of pine charcoal in a top-lit downdraft moving-hearth gasifier. Fuel 2014;118:27–32.
[25] Peters L, Hussain A, Follmann M, Melin T, Hägg MB. CO_2 removal from natural gas by employing amine absorption and membrane technology—A technical and economical analysis. Chem Eng J 2011;172:952–60.
[26] Shabbar S, Janajreh I. Thermodynamic equilibrium analysis of coal gasification using Gibbs energy minimization method. Energy Convers Manag 2013;65:755–63.
[27] Michiel JAT, Andre PCF, Carlo NH, Martijn RMVH. Exploration of the possibilities for production of Fischer Tropsch liquids and power via biomass gasification. Biomass Bioenergy 2002;23:129–52.
[28] Melgar A, Pérez JF, Laget H, Horillo A. Thermochemical equilibrium modelling of a gasifying process. Energy Convers Manag 2007;48:59–67.
[29] Channiwala SA, Parikh PP. A unified correlation for estimating HHV of solid, liquid and gaseous fuels. Fuel 2002;81:1051–63.

Nomenclature

ΔH^0_r: Heat of reaction at standard condition 298 K (MJ/kmol)
CO_2 EMR: CO_2 emission ratio (–)
CO_2/C: Mole of CO_2 as reaction agent per mole of carbon in biomass (–)
$H^0_{i,298}$: Heat of combustion of ith component in syngas product (MJ/kmol)
L_{298}: Latent heat of vaporization of water at standard condition 298 K (MJ/kg)
M_H: Mass flow rate of atomic hydrogen in biomass (kg/h)
M_i: Mass flow rate (kg/h)
n_i: Molar flow rate of ith component in syngas product (kmol/h)
O_2/C: Mole of O_2 as reaction agent per mole of carbon in biomass (–)
S/C: Mole of steam as reaction agent per mole of carbon in biomass (–)
x_C, x_H, x_O: Mass fraction of carbon, hydrogen and oxygen in biomass (–)
y_{CH4}: Mole fraction of CH_4 in product gas (–)
y_{CO}: Mole fraction of CO in product gas (–)
y_{CO2}: Mole fraction of CO_2 in product gas (–)
y_{H2}: Mole fraction of H_2 in product gas (–)

Abbreviations

BD: Boudouard reaction
CBGR: Combined biomass gasifier and reformer without CO_2 recycled
CBGR-Post-reCO_2: Combined biomass gasifier and reformer with Post-CO_2 recycled
CBGR-Pre-reCO_2: Combined gasifier and reformer with Pre-CO_2 recycled
CGE: Cold gas efficiency (–)
Con-BG: Conventional biomass gasifier without CO_2 recycled
Con-BG-reCO_2: Conventional biomass gasifier with CO_2 recycled
CR: CO_2 reforming
GSE: Gasification system efficiency (–)
HHV: Higher heating value (MJ/kg)
LHV: Lower heating value (MJ/kg)
MF: Methane formation
MR: Methane reforming
PO: Partial oxidation
rWGS: Reverse water gas shift
SR: Steam reforming
WGS: Water gas shift